ENHANCING PERFORMANCE OF MATERIALS IN TURBOMACHINERY: A REVIEW OF COATING AND SURFACE MODIFICATION TECHNOLOGIES

by
Scot Laney
Materials Engineer
and
Derrick Bauer
Materials Engineer
The Elliott Group
Jeannette, Pennsylvania

Scot Laney is a Materials Engineer with The Elliott Group, in Jeannette, Pennsylvania. He joined Elliott Group in 2007, and has been involved with materials related R&D projects, failure analysis, and aftermarket support. He also has experience in the areas of high temperature oxidation/corrosion and protective coatings.

Dr. Laney received his B.S. degree (2001), M.S. degree (2004), and Ph.D. degree (2007) from the University of Pittsburgh in Materials Science and Engineering. He is also a member of ASM.

Derrick Bauer is a Materials Engineer with The Elliott Group, in Jeannette, Pennsylvania. He joined Elliott Group in 2002, and has been involved with materials related R&D projects, failure analysis, production and aftermarket support, and remaining life assessments.

Mr. Bauer received his B.S. degree (2002) from the University of Pittsburgh and is currently working toward his M.S. degree from the same institution.

ABSTRACT

Despite best efforts in choosing a suitable alloy, it is frequently impossible to find a single material that is ideal for the particular application in a centrifugal compressor or steam turbine. In these situations, a coating may be used to exploit the beneficial properties of two or more materials for the purposes of enhancing a particular property for service under specific conditions or reducing the cost by allowing for the use of less expensive substrate material, among other reasons. Coatings are often designed to be multifunctional so they can address multiple problems simultaneously. Centrifugal compressors in the petrochemical industry and steam turbines offer several opportunities for the use of coatings due to the often harsh and changing conditions of the process. This paper discusses several commonly encountered issues and how coatings can be used to mitigate them by maintaining design performance for longer periods and reducing the cost of maintenance associated with these problems.

INTRODUCTION

The turbomachinery industry is a mature industry with roots that trace back over a century. Over this history, original equipment manufacturers (OEMs) have developed tried and true designs manufactured from proven materials. Given the successes, customers have come to expect reliability and longevity from their equipment. The challenge for the OEMs is then how to utilize these designs in ever more severe applications while meeting customer expectations associated with equipment performance and reliability. Despite best efforts in choosing a suitable alloy, it is frequently impossible to find a single material that is ideal for the particular application. In this case, coatings may be used to exploit the beneficial properties of two or more materials. Coatings have been applied to the rotating and stationary components of both centrifugal compressor and steam turbines to enhance performance in a number of areas, including resistance to corrosive environments, minimizing the rate of solid particle erosion and liquid droplet erosion, and improving the foulant release ability of the component, among others. This paper will discuss the properties and application methods of various coating systems for centrifugal compressor and steam turbines to prevent corrosion, fouling, erosion, and improve the wear resistance.

CORROSION

Corrosion is a common problem in many industries, and centrifugal compressors operating in the petrochemical industry are certainly no exception. Corrosion is an electrochemical attack that can occur as an even attack on the surface of the material (general corrosion) or an uneven, localized attack (pitting), as well as lead to selective attacks such as stress corrosion cracking. While there are numerous corrosion mechanisms, for the purposes of this paper, they will be simplified into these general areas. The reader is directed to the multitude of information available in the literature for a more in-depth discussion on the topic. In order to help prevent corrosion, coatings are applied to act as a barrier between the substrate and the environment. Typically, the coating is a sacrificial layer with slower reaction kinetics than the substrate material in the particular environment.

In many cases, suitable corrosion protection can be obtained by changing the component material to a more corrosion resistant material such as stainless steel. Corrosion is usually accompanied by other damage mechanisms such as fouling or erosion. Because of this fact, few coatings are applied solely for the prevention of corrosion. Fouling will be discussed later in this paper, but successful antifouling coatings must provide corrosion protection in the particular environment. A similar statement can be made for erosion coatings (Wang, et al., 2003).

Corrosion is an important consideration, as it can significantly reduce the fatigue life of a particular component. While it is detrimental, general corrosion does not often play a large role in fatigue failures in most centrifugal compressor and steam turbine environments. On the other hand, pitting corrosion has a particularly negative effect on the fatigue life since it can create atomically sharp cracks on the surface of the component. This will act as a stress riser, which is a perfect initiation site for fatigue cracks.

Since fatigue cracks spend most of their life in the initiation phase, corrosion pits help the fatigue crack quickly initiate and begin the propagation phase. Figure 1 is a plot showing the negative effect of corrosion on fatigue resistance.
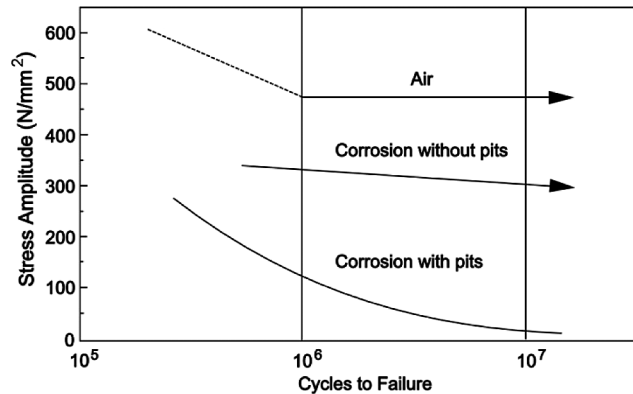

Figure 1. Plot Showing the Effect of Corrosion on Fatigue Life (Dowson, et al., 2008).

Compressors

Phenolic coatings are one such coating that has been successfully applied solely for corrosion protection. Figure 2 shows a compressor rotor coated with one such coating. Baked phenolic coatings have shown excellent resistance to solvents, acids, salts, and mildly alkaline solutions, making it very useful for corrosion protection in the petrochemical industry. Phenolic coatings are sprayed as a liquid or dipped and require a subsequent baking at an elevated temperature. During the baking procedure, the rotor must be hung in the vertical position to maintain the dimensional integrity. This phenolic coating is an option in certain situations where it will perform better than stainless steel or where the increased price of using a stainless steel component cannot be justified by the end user (Heresite Protective Coatings Inc., 1999).
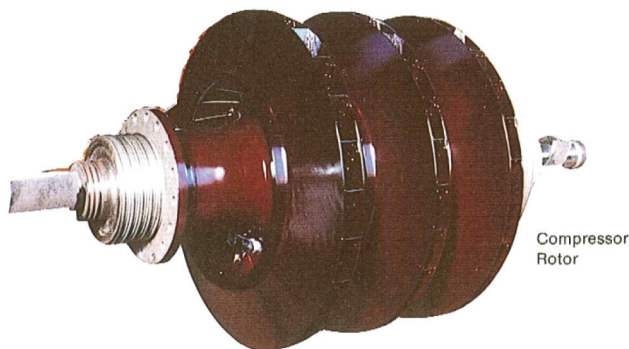

Figure 2. Compressor Rotor with Phenolic Coating (Heresite Protective Coatings Inc., 1999).

Two coating systems that have been applied to centrifugal compressors for corrosion protection are composite coatings with organic top layers and electroless nickel. Both coatings are normally applied for their antifouling properties, however, providing superior corrosion protection is a prerequisite for an effective antifouling coating. Electroless nickel coatings are especially effective in chlorine environments, caustic environment and hydrogen sulfide environments. Both of these coatings will be discussed in-depth in the next section of this paper.

Weld overlays can be used to apply a corrosion-resistant alloy to the surface of a less corrosion resistant alloy. This process has been used on casings in which an AISI 309 stainless steel alloy was overlayed on a carbon-steel casing at the O-ring areas. These areas of a casing are critical since a general corrosion attack could

increase the O-ring groove depth. Overlays have also been applied to the seal areas of critical components such as impellers. The advantage of using weld overlays is that a corrosion-resistant alloy can be applied to localized, critical areas of a large component that can be much more cost effective than making the entire component from a more expensive alloy. Figure 3 is an image of a casing with AISI 309 overlaid in the O-ring grooves in the outer barrel in acid gas service.
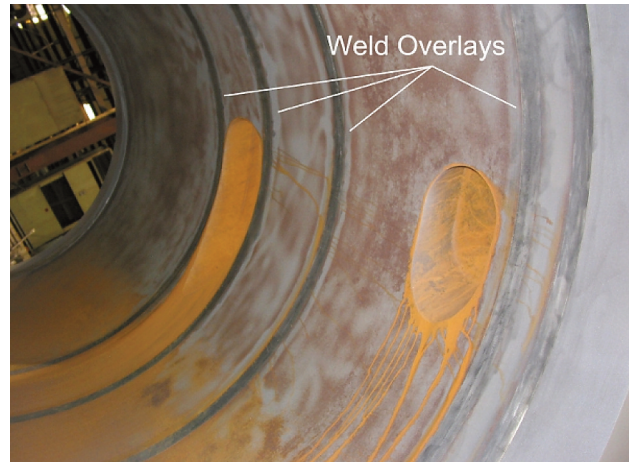

Figure 3. Picture of AISI 309 Weld Overlays on O-Ring Grooves of an Outer Casing.

For selection of materials for sour gas service, API 617 (2002) refers to NACE MR0103 (2002) and MR 0175/ISO 15156 (2003). No coatings are approved by NACE MR0103 or MR0175/ISO 15156 for standalone protection against stress corrosion cracking, but coatings are still allowable for general corrosion resistance. Both NACE MR0103 and NACE MR0175/ISO 15156 specify grades of steel and their respective heat-treated condition necessary for resisting stress-corrosion cracking. Even when a coating is applied to a substrate, the substrate material must meet the requirements of the above specifications. With any coating, there is always a risk that the coating will be removed at a small location, either by erosion, localized pitting or foreign object damage, which will expose the substrate to the corrosive environment. Metallic, electrolytic coatings contain microscopic cracks that will allow the H_2S to contact the substrate surface. Hydrogen sulfide can diffuse through polymer coatings to reach the substrate while thermal spray coatings are porous and will not provide adequate protection.

Steam Turbines

Under ideal conditions, corrosion is not a significant concern in steam turbines. Stainless steel materials perform extremely well without coatings in an elevated temperature steam environment. The turbine blade material is typically a 400 series stainless steel, such as AISI 403 or AISI 422 stainless steel. These steels will form a thin layer of Cr_2O_3, which is a very stable oxide and has a slow growth rate. This oxide serves as a barrier between the environment and the base metal and prevents further oxidation of the blades. The Cr_2O_3 creates an effective barrier because the inward and outward diffusion of atoms through the Cr_2O_3 layer is extremely slow.

Corrosion becomes a problem when there is an underlying problem with the process, and this is normally the result of impure steam. Impure steam carries with it elements that increase the corrosion process. Typically, the amount of impurities in the steam is not large enough to change the general corrosion rate; rather they cause localized attack that leads to pitting. A photomicrograph of a corrosion pit is shown in Figure 4. The tip of the corrosion pit creates a stress riser, which is an ideal location for an initiation site of a fatigue crack (Dowson, et al., 2008). An earlier figure in this

paper (Figure 1) already illustrated the negative impact corrosion has on the fatigue life of a component. Pitting corrosion does not commonly occur on stainless steel components when the steam quality meets NEMA SM-23 (1991) requirements (Table 1) as referenced by API 612 (2005).
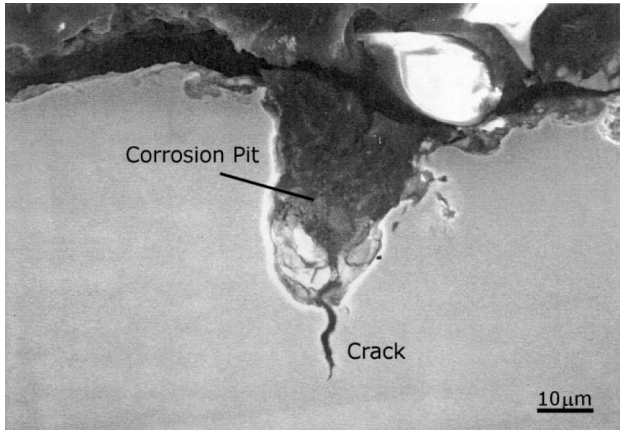

Figure 4. Photomicrograph of a Corrosion Pit (Dowson, et al., 2008).

Table 1. NEMA SM-23 Steam Purity Quality Requirements.

	Continuous	Start-Up
Conductivity, micromhos/cm at 25℃		
Drum	0.3	1
Once Through	0.2	0.5
SiO, pbb, max	20	50
Fe, pbb, max	20	50
Cu, pbb, max	3	10
Na+K, pbb, max		
Up to 800 psi [5516 kPa (gauge)]	20	20
801 to 1450 psi [5517 to 9998 kPa (gauge)]	10	10
1451 to 2400 psi [9999 to 16548 kPa (gauge)]	5	5
Over 2400 psi [over 16548 kPa (gauge)]	3	3

Similar to compressors, there are not many coatings applied to steam turbine components solely for corrosion prevention. If there are problems with corrosion, usually other problems are occurring, such as erosion or fouling, which also must be addressed by a coating. A few coatings that have been used for corrosion prevention will be discussed.

Diffused chromium coatings have proven to be effective in helping to prevent corrosion. During this process, chromium is diffused into the surface of the component by a pack cementation process or chemical vapor deposition (CVD) in order to locally increase the chromium concentration at the surface. This helps to ensure that a continuous Cr_2O_3 layer is maintained during service. As previously stated, this coating is mainly used to help prevent pitting corrosion.

One coating that has been used by OEMs for minimizing the corrosion on steam turbine blades is a titanium nitride topcoat with a chromium undercoat (Figure 5). This coating system, applied by a physical vapor deposition (PVD) process, produces a chromium coating on the surface of the substrate. This chromium layer provides excellent corrosion protection for the substrate and acts as a bond layer for the titanium nitride topcoat. It also provides a relatively soft undercoat for the topcoat. This chromium undercoat has a thickness of 13 microns and has a hardness of 440 HV on the 0.5 kg scale. The titanium nitride topcoat only has a thickness of 2 microns with a hardness of 1880 HV on the same 0.5 kg scale. This coating system is stable at all operating temperatures of the steam turbine, so it can be applied to all rows of blades. The titanium nitride topcoat is a strongly bonded ceramic and is inert in a steam atmosphere (Ebara, et al., 1987).

Figure 5. Picture of Titanium Nitride Coated Blade.

Another coating that may be used for minimizing the corrosion of steam turbine components is an amorphous nickel coating. This coating will be described in the next section of this paper since corrosion pitting is often the result of foulant buildup on the turbine blades.

FOULING

Fouling is a common problem in compressors. Fouling refers to the buildup of solids, usually polymeric materials, on the internal aerodynamic surfaces of the machine (Dowson, et al., 2008). While it does not usually lead to catastrophic failure, it does gradually reduce the efficiency of the machine by increasing the mass of the rotor, altering the aerodynamics, and blocking flow paths. If left unchecked, fouling can block the flow path to the extent that production is stopped or cause imbalances that can damage the machine. Figure 6 shows examples of fouling in various services. Depending on the service, fouling substances may come from outside of the machine or be generated internally. External foulants may come from airborne salt, submicron dirt, and organic or inorganic pollutants in the process gas. In petrochemical compressors, the situation is much more complicated, as the foulants can be generated internally. For example, in ethylene cracked gas compression, fouling results from the polymerization reactions intrinsic to the compression process. The conditions that lead to this type of fouling can be variable from service to service or even machine to machine in the same service.

Figure 6. Examples of Fouling of Centrifugal Compressors in Various Services.

The details related to the fouling are also often not understood or considered proprietary to the end users process, which makes the determination of the need and effectiveness of an antifoulant coating difficult. Basic information related to the compressor such as size, parts to be coated (rotor and/or diaphragms), material type, and if/what coatings are currently on the parts is easily collected information that should be provided to the coating applicator. Service related information is usually more difficult. This can include the general type of service, gas analysis, pH of the gas, temperatures, and pressures. Information related to the washing practices are also vital, this can include the method of injection, the type of fluid used, and the rate. Frequently, if an antifoulant coating

fails, it is due to improper evaluation of the above parameters by the applicator and/or the customer or a process upset occurs that unfavorably shifts the parameters.

Foulant release coatings are relatively new to the turbomachinery industry, with the first application (to the knowledge of the authors) in late 1970s. Testing had begun of various coatings for foulant release during the middle part of the decade (Sturley and Moore, 1982). This work culminated in a stratified fluoropolymer coating that was applied in a single layer to the cast iron diaphragms of an ethylene compressor with foulant issues in 1978-79. The coating performed well on the diaphragms, but led to the foulant being transferred to the uncoated rotor and resulted in decreased clearances. The coating was removed accidentally from the diaphragms during cleaning and was not reapplied due to cost. By the latter part of the 1980s, a coating system was developed that forms the basis of the current organic antifoulant coatings. In a drastic departure from the organic coatings that were and continue to be prevalent in the industry, electroless nickel was found to perform well as an antifouling coating in the early part of the last decade (Wang, et al., 2003). More recently, durable antifoulant coatings for the latter stages of steam turbines have also been developed.

As can be ascertained from the history above, there are two types of foulant release coatings available for centrifugal compressors, i.e., organic and electroless nickel. Compared to the other coatings discussed in this paper, these coatings are probably the most complex and least understood in terms of how they work. The following will describe the structure, application methods, and some properties of these coatings.

The most commonly available antifoulant coating is the organic variety. Figure 7 shows an example of a compressor rotor coated with an organic antifoulant coating. The coating can consist of a single layer, similar to the stratified fluoropolymer mentioned above, or as many as four layers. Figure 8 is a schematic showing the structure of a three-layer coating. Figure 9 is a micrograph of a four-layer system. The under layers are added solely for corrosion resistance and to aid in adhesion of the top layer. They do not add to the foulant release properties of the coating. The base layer is an aluminum-filled chromate/phosphate layer applied by spray or dipping and subsequently baked to cure. Chromate/phosphate is an amorphous ceramic with excellent general corrosion and oxidation resistance. The term aluminum filled means that discrete aluminum particles are added to the chromate phosphate. The purpose of the aluminum is to provide sacrificial galvanic corrosion protection in the event the coating is compromised (Chow, et al., 1994). Aluminum is more active than steel, and will be preferentially attacked in a galvanic corrosion situation. Because the aluminum is present as discrete particles, the corrosion is limited to the particle or particles that are exposed by the indication in the coating. Although it is counterintuitive given the previous statement, this layer is frequently burnished to bridge the aluminum particles, which increases the conductivity of the coating and increases the corrosion resistance. A second layer of the chromate/phosphate can be added. Depending on the top coat, there might be an intermediate ion active organic primer/sealer layer. The primer acts as a corrosion inhibitor for the base coat(s) and helps with the adhesion of the top coat. This layer is also applied by a spray or dip and bake process. The top layer is a fluoropolymer resin, typically containing polytetrafluoroethylene (PTFE). This layer is also applied by a spray or dip and bake process, Tables 2 and 3 show some of the properties of PTFE. For this particular application, the high chemical resistance and low coefficient of friction are of importance. Both of these are related to the molecular structure of PTFE, which leads to a low surface energy. Low surface energy means that PTFE does not readily bond with anything in contact with it; therefore, it is difficult to attack chemically and attraction forces that prevent sliding are very low. It also means that PTFE is hydrophobic (water fearing) and oleophobic (oil fearing). When water, which has a higher surface energy, is in

contact with PTFE, the wetting angle, or angle between the PTFE/water interface and water/gas interface, is very large at approximately 108 degrees (Chessick, et al., 1956). The result is that water tends to pull itself into a nearly spherical shape or beads up on the PTFE. This is illustrated in Figure 10. The beads of water easily roll off the surface. Oil has a lower surface energy than water. This results in a lower wetting angle and oil tends to spread out more, but still beads on a PTFE surface. As can be imagined, liquid precursors to solid foulants are not able to adhere to the surface and fouling is difficult to initiate on a PTFE containing surface. Figure 11 shows the performance of foulant release coatings, including two organic coatings with PTFE top coats, in terms of mechanical removal of a foulant by scrubbing against a commercially available nylon web pad alternative to steel wool. The foulant, formally called "gunk," was applied to coated samples and baked on. The samples were then scrubbed against the nylon scrub pad, and the number of cycles necessary to remove the gunk from the samples was counted. The fewer cycles necessary to remove the gunk, the better the antifouling properties of the coating are considered to be.

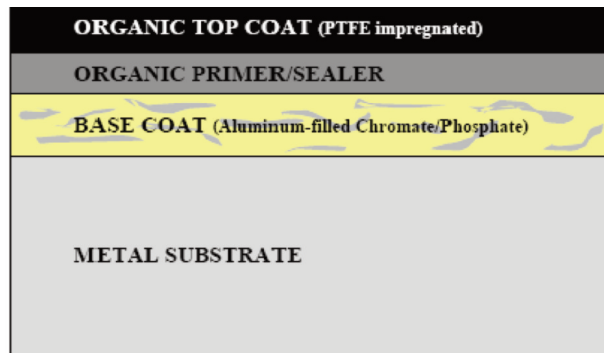Figure 7. Centrifugal Compressor Rotor Coated with an Organic Antifoulant Coating (Dowson, 2007).

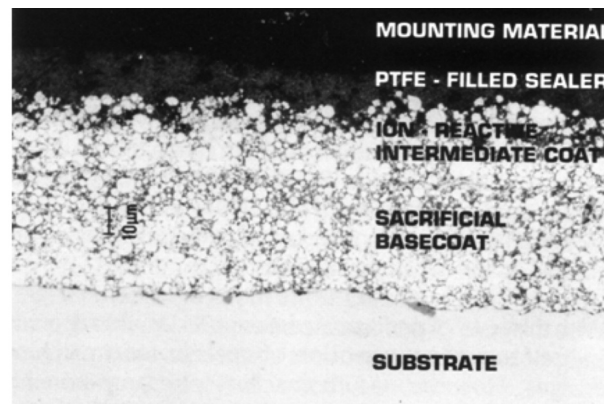Figure 8. Schematic of a Three Layer Coating System (Wang, et al., 2003).

Figure 9. Micrograph of a Four Layer Coating System (Chow, et al., 1994).

Table 2. Mechanical Properties of Various Fluoropolymers (after Fluoropolymer Comparison—Typical Properties).

Property	ASTM Standard	Unit	PTFE	FEP	PFA	ETFE
Specific Gravity	D792	---	2.15	2.15	2.15	1.76
Tensile Strength	D1457 D1708 D638	MPa (psi)	21-34 (3000-5000)	23 (3400)	25 (3600)	40-46 (5800-6700)
Elongation	D1457 D1708 D638	%	300-500	325	300	150-300
Flexural Modulus	D790	MPa (psi)	496 (72000)	586 (85000)	586 (85000)	1172 (170000)
Folding Endurance	D2176	(MIT) cycles	$>10^6$	$5\text{-}80\times10^6$	$10\text{-}500\times10^6$	$10\text{-}27\times10^6$
Impact Strength	D256	J/m	189 (3.5)	No Break	No Break	No Break
Hardness	D2240	Shore D pencil	50-65 HB	56 HB	60	72
Coefficient of Friction, Dynamic	D1894	---	0.5-0.10	.08-0.3	---	0.3-0.4

Table 3. Chemical Resistance of Various Fluoropolymers (after Fluoropolymer Comparison—Typical Properties).

Property	ASTM Standard	Unit	PTFE	FEP	PFA	ETFE
Chemical/Solvent Resistance	D543	---	Excellent	Excellent	Excellent	Excellent
Water Absorption, 24h	D570	%	<0.01	<0.01	<0.03	<0.03
Salt Spray Resistance[1]	B117					
-on aluminum		Hours	744+	744+	1000	1000
-on steel		Hours	192	---	---	---
Detergent Resistance[2]	---					
-on aluminum		Hours	264	744	---	---
-on grit-blasted aluminum		Hours	624	600	---	---
-on grit-blasted steel		Hours	24	480	---	---
Weather Resistance	Florida Exposure	Years Unaffected	20	20	10	15

[1] Salt Spray Resistance, 5% NaCl at 35°C/95°F, hours to failure
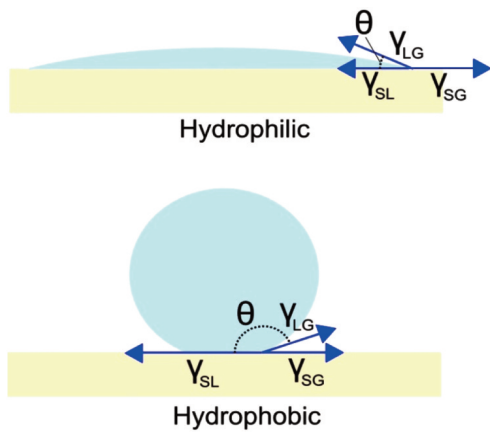[2] Detergent Resistance, hours to failure

Figure 10. Schematic Illustrating Wetting Angle Concept.
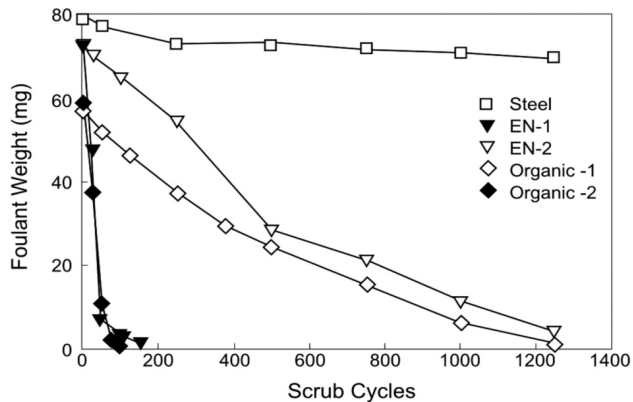

Figure 11. Plot Showing Remaining Weight of Foulant Versus Scrub Cycles for Various Antifoulant Coatings (Wang, et al., 2003).

Despite the numerous positive aspects of the coating, there are some disadvantages. The coating structure is complicated with multiple layers and various types of materials, i.e., polymers, metals, and ceramics. For coatings in general, using various material types and layers yields a mishmash of properties and typically leads to problems such as reduced adhesion or cracking. Multiple layers can also increase the overall variability between different locations in the coating and between the coatings on different components. This is particularly true when it is considered that the application methods are prone to variability in thickness and coverage. Another downfall of this coating is that it has been shown to have poor resistance to some washing practices (Wang, et al., 2003). Washing fluids are often injected into compressors for several reasons, including to aid in the removal of foulants. These fluids can be water/steam or oil and can contain detergents or solvents. A number of instances have been reported where the injection has lead to the deterioration of the coating, whether by erosion of the relatively weak PTFE layer, by chemical attack, by blistering, or by a combination of two or more of these. The removal by erosion can occur if the wash liquid is not properly introduced into the compressor and leads to liquid droplet erosion. Coating removal by erosion can also happen by solids or liquids in the gas in the absence of injections. Chemical attack can occur if the pH is outside of the suggested range (4-9) or if a solvent forms in the compressor that the PTFE layer is not resistant to, such as amines. Blistering can occur if a chemical is able to penetrate or is absorbed by the coating and is then vaporized. Wang, et al. (2003), discuss this occurring in a case study with benzene being absorbed by the coating and steam injections causing it to vaporize. Figure 12 shows some images from this case study with examples of chemical attack and blistering. This reiterates the need to divulge as much information as possible about the compressor environment and operation upfront, so the coating applicator can determine if the coating is likely to survive.
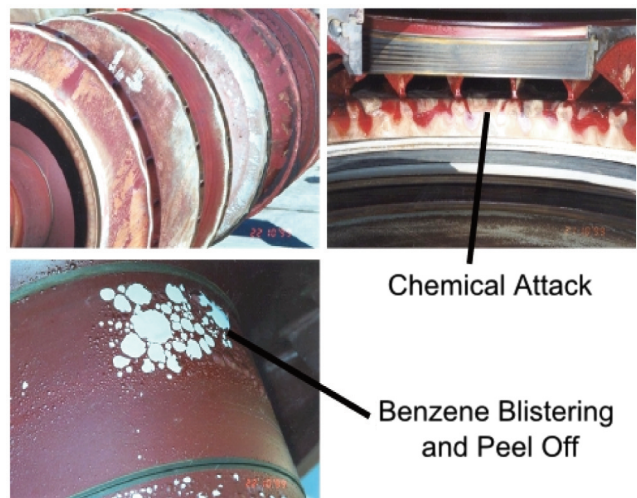

Figure 12. Images Showing Degradation of Organic Coating after Two Years of Service.

While electroless nickel has just recently been applied for foulant release purposes, it has a history in the turbomachinery industry as a corrosion resistant coating. Figure 13 shows the gas path of an impeller coated with electroless nickel before service. Figures 14 and 15 shows a rotor after five years of operation in the same service as the coating in Figure 12. As illustrated in Figure 11, the testing shows that foulant release is nearly identical to that of the organic type coatings. The similarities between the two types of coatings end there.

Figure 13. Image Showing Gas Path of a Centrifugal Compressor Impeller Coated with Electroless Nickel.
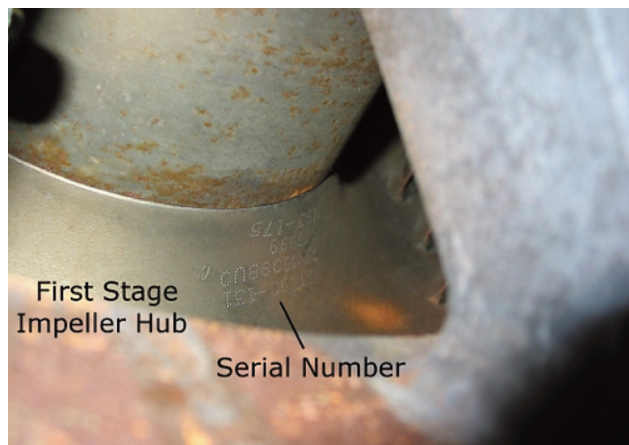

Figure 14. Photo Showing an Electroless Nickel Coated Impeller Hub after Five Years Service.

Figure 15. Photo Showing an Electroless Nickel Coated Rotor after Five Years Service.

Electroless nickel is applied by an autocatalytic chemical reduction of nickel ions by hypophosphate (Baudrand, 1994). In more simple terms, a nickel-phosphorus alloy coating is deposited by a chemical reaction between a nickel containing solution and a hypophosphate solution. The deposition does not require an outside electrical current. In practice, the surface condition of the parts is critical to optimal coating properties. The actual coating process therefore consists of dipping the parts in a series of acidic and caustic cleaning baths prior to the final dip into the nickel bath. Figure 16 shows an overhead view of an electroless nickel plating

facility. The chemistry of the coating bath determines the amount of phosphorus in the coating and the main variable in determining the coating thickness is time. The fact that the parts are dipped into a coating bath makes the process amenable to complex shapes. This also led to one previous downfall of the coating. When applying the coating to rotors, the chemicals can easily penetrate the gaps between rotor components. This can lead to poor coating adhesion around the gap, unseen corrosion if the chemical is trapped for any period of time, and can reduce thermal gaps if the electroless nickel plates in the gap. In the past, this was addressed by coating the rotor components separately before building the rotor. Recently, a method for addressing this has been developed and has successfully applied the coating to rotors from two horizontally split, multistage 60M centrifugal compressors (Laney and Walker, 2009).
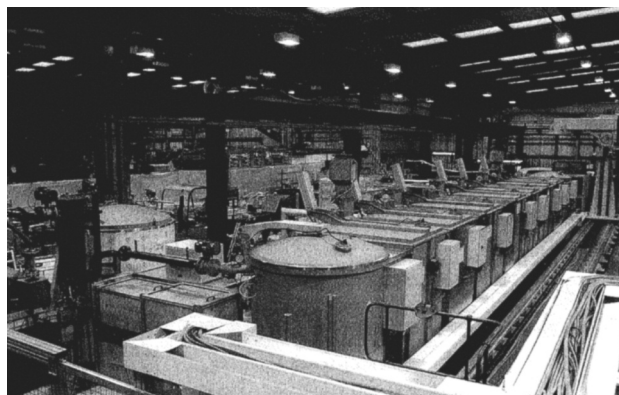

Figure 16. Electroless Nickel Plating Facility.

Electroless nickel alloys are often broken down into low, medium, and high phosphorus contents with each range having slightly different properties and behaviors. For antifoulant applications, high phosphorus electroless nickel, containing 10 to 14 percent P, is used. The high phosphorus content makes electroless nickel a rather unique material. High phosphorus electroless nickel deposits as a continuous film and with a very uniform coating thickness (Figure 17). Electroless nickel is one of the few engineered metallic glasses in common usage (Baudrand, 1994). Metals have long range order at the atomic level and are therefore characterized by their crystal structure. The atomic structure of metallic nickel, for example, can be reduced down to a single cube with atoms at the corners and in the faces. This is called the face centered cubic (fcc) crystal structure (Figure 18). On the other hand, glass is amorphous, meaning it has no long range order and no identifiable crystal structure (Figure 19). A metallic glass is a combination of these two and is therefore a metal that has no long range order. Similar to glass, metallic glasses typically have excellent corrosion resistance, due to the lack of grain boundaries and the difficulty of diffusion occurring in the amorphous structure. Electroless nickel is no exception with a substantial list of chemicals that it is resistant to. The glass-like nature also instills strength and hardness to the coating, which allows electroless nickel to perform well in wear applications. The effect of phosphorus on the tensile strength is shown in Figure 20. Although it is more common with the low phosphorus variety, electroless nickel has been used as a replacement for hard chrome in wear applications. The wear properties can be increased by heat treatment (Figure 21), but that typically causes a reduction in some of the other properties related to fouling resistance. Despite the glassy nature, electroless nickel does have some toughness and ductility, which is shown in Figure 22. The combination of corrosion resistance, strength, hardness, and ductility allows electroless nickel to withstand washing media injected into the machine. Phosphorus also has some natural lubricity and gives electroless nickel a low coefficient of friction. The combination of phosphorus and the amorphous structure is what results in the excellent release properties. Finally, it also has excellent

adhesion to the substrate. In fact, the electroless nickel coatings are often required to pass a 180 degree bend test outlined in ASTM E290 and can pass other adhesion tests outlined in ASTM B571.

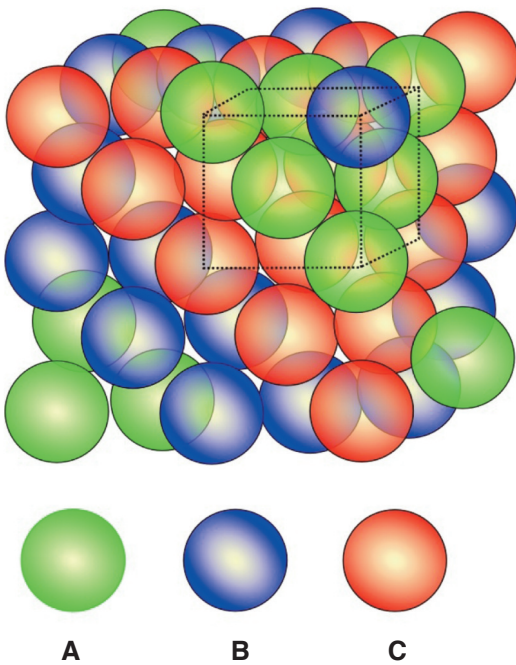Figure 17. Cross-Section of an Electroless Nickel Coating (Electroless Nickel Plating).

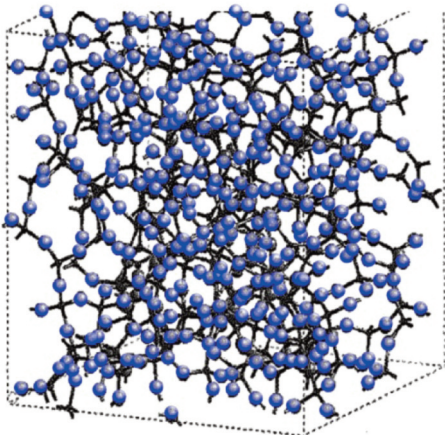Figure 18. Model Showing the FCC Crystal Structure (after Allen and Thomas, 1999).

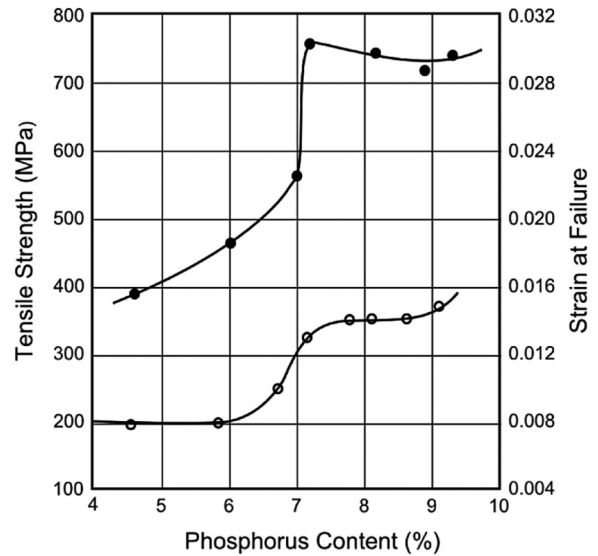Figure 19. Model Showing the Amorphous Structure of Silica Glass (after Allen and Thomas, 1999).

Figure 20. Plot Showing the Effect of Phosphorus on Tensile Strength of Electroless Nickel (Graham, et al., 1965).
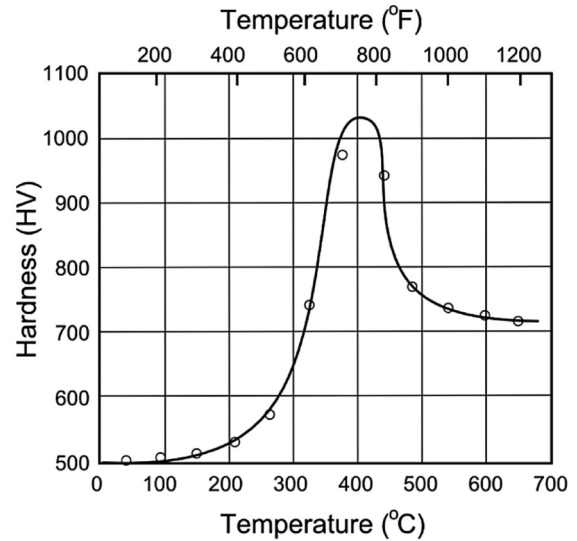
Figure 21. Plot Showing the Effect of Heat Treatment Temperature on Hardness of High Phosphorus Electroless Nickel (Gawrilov, 1979).
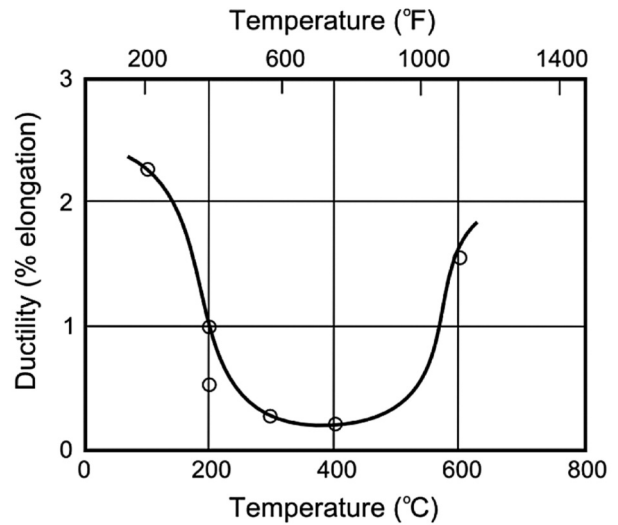
Figure 22. Plot Showing the Effect of Heat Treatment on Ductility of Electroless Nickel Coatings (Baldwin and Such, 1968).

There also some disadvantages to electroless nickel coatings. The coating can have internal stress in it when applied. Figure 23 shows that this stress can change from tensile to compressive depending on the phosphorus content. For high phosphorus electroless nickel, the stresses are slightly compressive. Compressive stresses in a coating can be beneficial to the coating for resistance cracks, among other things. Unfortunately, the compressive stress in the coating must be balanced by a tensile stress on the base metal surface. As the coating gets thicker, the influence of the coating properties gets stronger, which results in a decrease in the crack resistance of the substrate with increasing coating thickness. This is illustrated in Figure 24. This effect can be controlled by surface treatments that impart a compressive stress in the substrate before coating. Compressor impellers, for example, are post weld heat treated and overspeed tested, which puts the high stressed areas in compression. These compressive stresses can nullify the tensile stresses due to the coating. A second disadvantage is related to the corrosion resistance of the coating and may be more of a perceived disadvantage than a legitimate concern. Electroless nickel is more passive than the low alloy steels that it is most frequently applied to. If the coating is penetrated during service or has defects from the application process, this can lead to galvanic corrosion of the substrate (Garverick, 1994). Although this is a problem, the likelihood and severity of the corrosion can be called into question. Several aspects of high phosphorus electroless nickel, such as adhesion, hardness, uniform deposition, reduce the likelihood of the coating being compromised. The corrosion product formed by the substrate will be iron oxides, which are not typically soluble in common media. This means that any pores that do form will be rapidly plugged with the corrosion product, causing a loss of contact between the electrolyte and the base metal. This effectively shuts off the galvanic corrosion mechanism (Arney, et al., 1985). A final consideration is that it is common practice in the turbomachinery industry to mix and match materials. Rotors, as an example, can have stainless steel impellers and sleeves on a low alloy steel shaft. In electrolytes that are representative of a centrifugal compressor environment, electroless nickel often lies in between AISI 410 stainless steel and carbon steel (low alloy steel should be similar) on the galvanic series. Given this, it would be expected that failures and other issues due galvanic corrosion would be rampant in the industry. To the contrary, the authors' are not aware of any failure of a centrifugal compressor due to galvanic corrosion. Finally, electroless nickel is more difficult to repair than the organic coatings. Typically, only the coating on the outside of impellers has required repair due to balancing. In these cases, brushed nickel, which is a portable electrolytic process, is used. There is a portable electroless nickel process for localized areas that has recently become available that may serve as a replacement for brushed nickel (Piper and Wang, 2007).
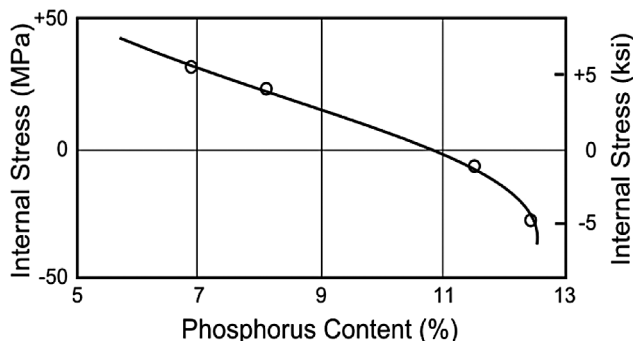

Figure 23. *Plot Showing the Effect of Phosphorus Content on Internal Stress of Electroless Nickel Coatings (Parker and Shah, 1971).*
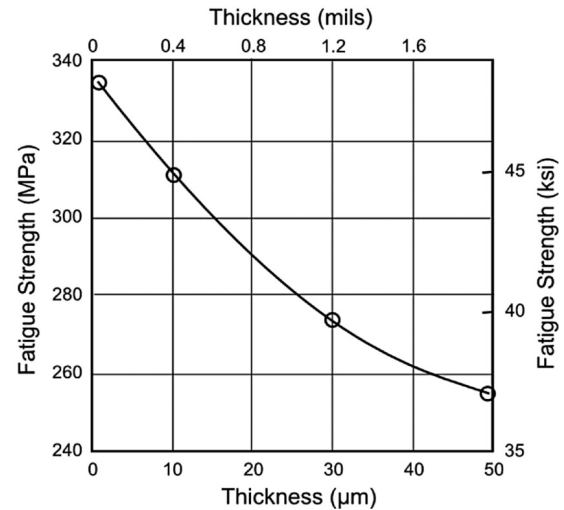

Figure 24. *Plot Showing Effect of Electroless Nickel Coating Thickness on Fatigue Strength of Carbon-Manganese Steel Substrate (Stallman and Speckhardt, 1981).*

Steam Turbines

Fouling and corrosion can also be a problem in steam turbines, not only causing corrosion damage but also can gradually reduce the efficiency of the turbine. Industrial turbines, whether condensing or noncondensing, can encounter problems with deposits building up on the turbine airfoils. In a turbine, hydroscopic salts, such as sodium hydroxide, can absorb moisture when superheated steam becomes saturated and condenses in the latter stages of the turbine. This condensation occurs when the steam passes through what is referred to as the Wilson Line. Wet sodium hydroxide has a tendency to adhere to turbine metal surfaces and can entrap other impurities such as silica, metal oxides and metal phosphates. Once these deposits have formed, they can be very difficult to remove. Turbine deposits may be a cause of decrease in efficiency and possibly an increase in vibration. A smooth, clean steam path will not collect deposits as easily as a dirty, already contaminated surface. Consequently, the condition of the metal surfaces will be a critical factor because an already contaminated surface will accumulate deposits more rapidly than a clean one. Therefore, it is desirable to prevent further deposit buildups and to remove the problems associated with the presence of the deposits by cleaning the turbine. Some OEMs have provided support to end users of turbines for water washing of steam turbines (Watson, et al., 1995). The effectiveness of the water removal procedures mainly depends on the adherence of the deposits to the substrate. Water washing is often undesirable since the operating speed of the turbine must be reduced as the blades impact the water droplets with a much greater force than steam. A surface aid that has superior antifouling or antistick properties combined with corrosion protection would be beneficial to the turbine blades in reducing the tendency for contaminants to stick to the blades and thereby improve the effectiveness of the water removal procedures (Wang, et al., 2003).

The titanium nitride topcoat with the chromium undercoat coating previously discussed will offer some antifouling benefits while minimizing the pitting corrosion that may occur on the surface of the component. The application of this coating provides a smoother substrate in comparison to machined turbine blade steel. A reduction in the surface roughness will limit the amount of deposits that build up on the airfoil. Impurities in the deposits, such as sulfur or chlorine, will not easily attack the TiN, which will reduce the pitting corrosion on the blades. Pitting will chemically bond the foulant to the surface of the blade, so the foulant will be easier to remove if the pitting does not occur.

Another option is to coat the surface of the blades with a material that has superior antifouling or antistick/corrosion characteristics. This in turn is beneficial to the turbine blades by reducing the tendency for

contaminants to stick to the blades and increase the effectiveness of any water washings performed on the rotor. An amorphous nickel coating system has been developed, which is a corrosion resistant coating that provides excellent antifouling properties. The amorphous nickel alloy coating is designed for the latter stages of the rotor as this is the location where the deposit buildup is most severe (Wang, et al., 2003). The amorphous nickel coating system provides excellent corrosion resistance, which is a prerequisite for any antifouling coating. Testing of an AISI 403 stainless steel sample coated with the amorphous nickel system showed no evidence of corrosion after one month of exposure to a steam environment. Literature research on this coating shows that it easily passes over 1000 hours of ASTM B117 corrosion testing under a 5 percent salt solution. There is also documentation that indicates that the amorphous nickel coating provides excellent corrosion protection in wet chlorine environments and prevents pitting of the substrate material. Sodium and chlorine are two impurities often found in steam, so resistance to both of these elements is necessary for an effective steam turbine blade coating. Similar to the Cr-TiN coating system, preventing pitting on the surface of the blade airfoils will allow for easier removal of any foulant that builds up on the surface and helps prevent fatigue crack initiation sites.

The same foulant release testing described earlier in this paper for compressor coatings was repeated for the Cr-TiN coating and the amorphous nickel coating, and the results are displayed in Figure 25. The same foulant release testing was chosen because the "gunk" used as a foulant has been proven to accurately determine the foulant release ability of the coatings (Dowson, et al., 2008). The foulant was completely removed from the amorphous nickel coating after approximately 250 cycles, while the foulant took over 2000 cycles to be removed from the Cr-TiN samples. Both samples show a significant improvement in comparison to bare steel. In Figure 26, a comparison of the foulant remaining on the coated samples for both coatings is pictured after 250 cycles.
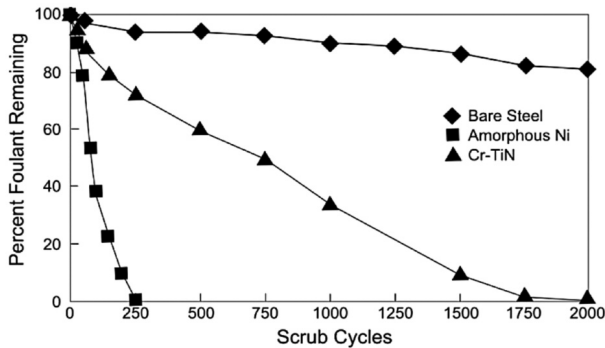

Figure 25. Results of Foulant Release Testing Performed on Turbine Blade Coatings (Dowson, et al., 2008).
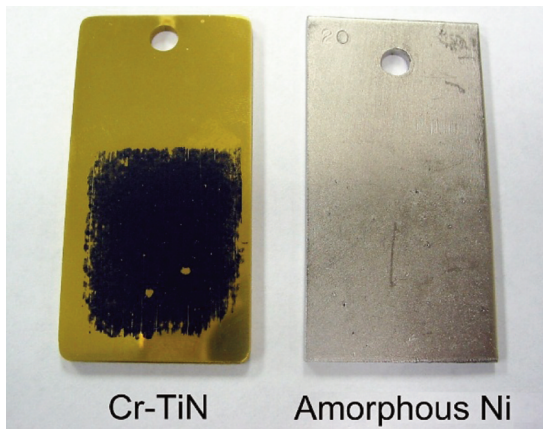

Figure 26. Comparison of Amorphous Nickel Coating Sample Against Cr-TiN Sample after 250 Cycles of Foulant Release Testing (Dowson, et al., 2008).

Cavitation erosion testing was performed to simulate liquid-droplet erosion as these conditions may occur during service. The amorphous nickel coating system and the Cr-TiN coating both experience minimal mass loss after 10 hours of erosion testing. An uncoated AISI 403 stainless steel in the quench and tempered condition acts as a control sample for this testing, and this sample did experience significant mass loss. The results of the cavitation erosion testing are given in Figure 27. It should be noted that although both coatings show resistance to cavitation erosion, their coatings are not a substitute for the application of Stellite® or tool steel to the leading edge of a turbine blade or the flame hardening of the leading edge for resistance to liquid droplet erosion. This testing was designed to evaluate the durability of the coating and to show that it is not easily removed from the turbine blade airfoil.
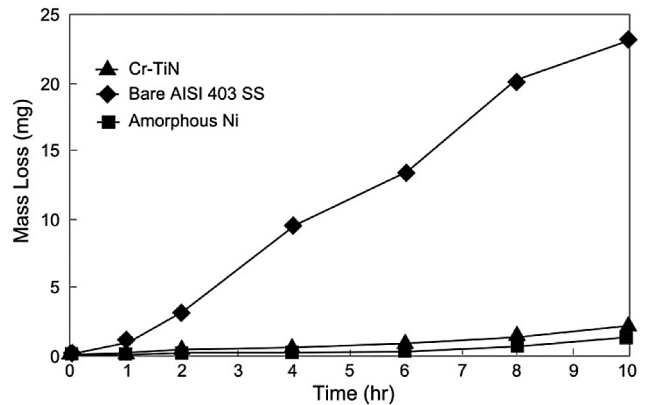

Figure 27. Comparison of Bare AISI 403 Stainless Steel Against Amorphous Nickel Coating and Cr-TiN Coated Samples after 10 Hours of Modified ASTM G32 Testing (Dowson, et al., 2008).

The results of fatigue testing performed on AISI 403 stainless steel samples and AISI 403 samples with the amorphous nickel coating system are given in Figure 28. Both the coated and uncoated samples reach their endurance limit of 10^8 cycles under a 55 ksi load. In order to prove the repeatability of the endurance limit, three consecutive samples were tested under the 55 ksi load. The results indicate that the amorphous nickel coating does not reduce the fatigue life of a turbine blade. The coating can also be applied to the blade root location for additional corrosion protection without altering the fatigue strength of the blade at this location.
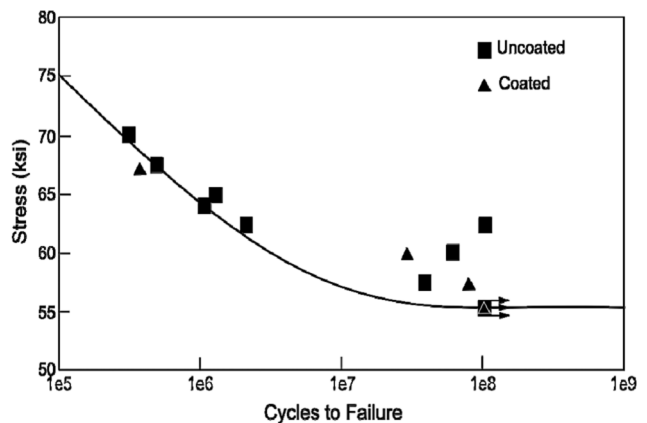

Figure 28. Results of R.R. Moore Fatigue Testing (Dowson, et al., 2008).

The amorphous nickel alloy coating is applied by a batch process, making it a more cost effective coating that can be provided with a shorter lead time (Figure 29). The amorphous nickel coating is applied at a thickness of 0.5 mils (13 microns). A method has been developed to apply the coating to a disk assembly; however, a process to coat the latter stages of a fully assembled rotor has not yet

been developed. Both the amorphous nickel coating and the Cr-TiN coatings are suitable for coating blades on new apparatus or at any point when reblading of the disk is necessary.
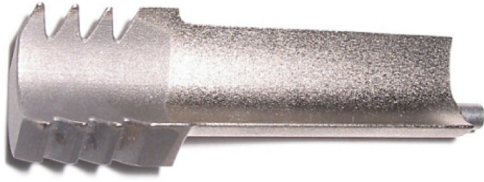

Figure 29. Picture of a Turbine Blade with Amorphous Nickel Coating.

WEAR

Sliding Wear

Damage to a solid surface can occur where there is a relative motion of two components that involve two contacting surfaces, generally involving a progressive loss of material. The hardness of a material is defined as the material's resistance to deformation. This is why hardness is measured by a standard indention on the surface of the material. By increasing the surface hardness of the material, the materials' resistance to deformation is increased, thus increasing the wear resistance of the material. This can occur in many locations on a steam turbine and a centrifugal compressor.

There are a number of possible solutions that have been used by turbine and compressor manufacturers for increasing the wear resistance of a component, including carburizing, nitriding, hard chromium coating and flame hardening.

During pack carburizing, carbon from the pack is diffused into the surface of the component (Figure 30). This is performed at an elevated temperature to increase the rate of diffusion. This can produce a case depth of up to 60 mils while producing a case hardness of approximately 55 HRC. This process can be performed on carbon steels and low alloy steels. The greatest advantage of pack carburizing is that it a relatively low-cost method of effectively hardening a material. The disadvantages of pack carburizing are that the case depth cannot be precisely controlled and burnishing of the surface is required after carburizing. Many times, only a minimum hardness at a minimum case depth is specified on a drawing. There are other methods of carburizing including gas carburizing, liquid carburizing and vacuum carburizing, which all provide better control of the case depth or produce a better surface finish, however these all have higher equipment costs and can be dangerous. Carburizing has been performed on guide pins to resist scoring during assembly, thrust disks, split nuts and on other components. The surface of the carburized samples is burnished to provide a smooth surface finish and decrease the coefficient of friction (Stickels, 1992).
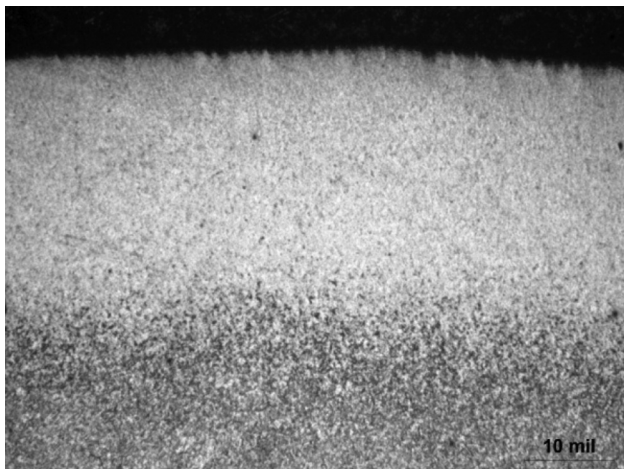

Figure 30. Photomicrograph of a Carburized Sample.

Gas nitriding introduces nitrogen into the surface of the steel that reacts with nitride formers within the steel such as aluminum, chromium, vanadium and molybdenum (Figure 31). The gas nitriding process is performed at approximately 535°C (1000°F), resulting in less distortion to the component in comparison to carburizing since no phase change of the material is involved. After gas nitriding, burnishing of the surface is required to provide a smooth surface finish and to remove a white layer that forms at the surface. Other forms of nitriding include salt bath nitriding and plasma (ion) nitriding (Maloney, 1992).
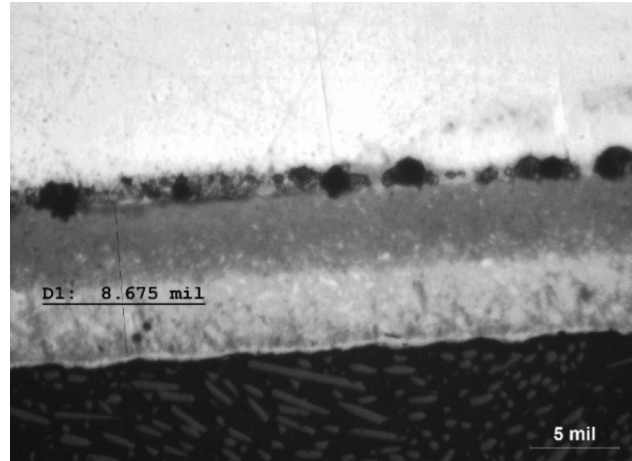

Figure 31. Photomicrograph of a Nitrided Sample.

Gas nitriding has been performed on guide bushings, washers, valve stem assemblies. Gas nitriding produces a case hardness similar to that of pack carburizing but at a reduced case depth (~10 mils). The main advantage of nitriding is that it can be performed on stainless steels as well as some carbon and low alloy steels.

A commonly used steel plating for reducing wear is a hard chromium plating (Figure 32). Plating thicknesses can vary between 2 microns and 15 microns. The plating thus provides a very hard surface (over 50 HRC), which helps increase the wear resistance. Another benefit of hard chromium coatings is that they can be applied to a localized area of a component. Hard chromium coatings have been successfully applied to both steam turbine shafts and compressor shafts in order to repair damaged or scratched areas.
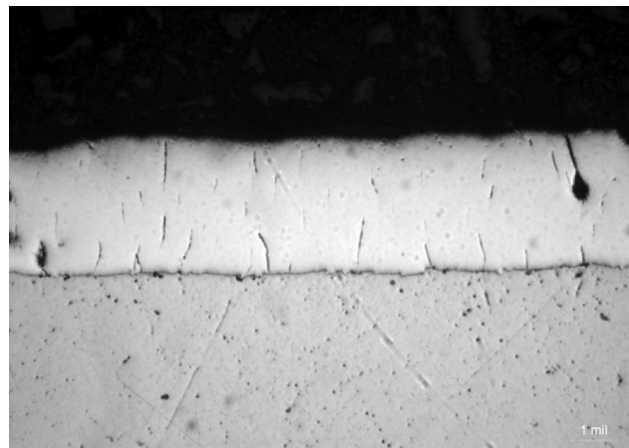

Figure 32. Photomicrograph of Hard Chromium Coated Sample.

Hard chromium plating may lead to hydrogen embrittlement of the substrate material during the plating process under certain conditions. If the coating is not properly applied, the plating may spall or flake during service, which may be detrimental to the component the plating is trying to protect.

Flame hardening involves the heating and rapid cooling of a hardenable material in order to increase the surface hardness. This method is commonly used hardening for many different components in a number of industrial applications, but it will be discussed in the next section since it applies to increasing the erosion resistance of turbine blades.

Erosion

Erosion, for the purposes of this discussion, will be defined as the redistribution and/or removal of material by repetitive, discrete impacts by either solid particulates or liquid droplets present in the process gas. The reasons for the distinction between solid and liquid erosive media will be discussed later. Erosion can lead to several problems. This includes, among other problems, degradation of component integrity, increased clearances, and changes in rotor dynamics. Even minor erosion can be a problem when it occurs as a precursor to or actively participates with other degradation mechanisms. For instance, surfaces roughened by erosion have a reduced fatigue endurance limit when compared to the virgin metal surface. Figure 33 shows a plot showing the effect of surface finish on the surface factor, which is used as a correction factor when calculating the endurance limit for a stress life analysis. Foulants also adhere more readily on eroded surfaces (Figure 34) and roughened surfaces can enhance corrosion rates through various mechanisms (Figure 35).
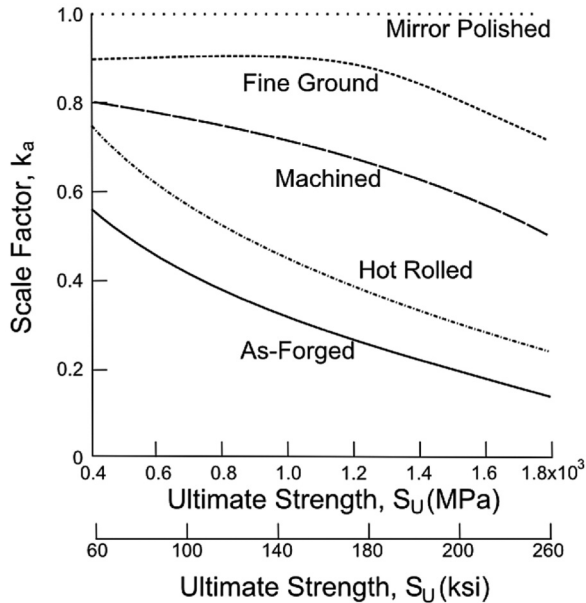

Figure 33. Plot Showing the Effect of Surface Finish on a Scale Factor Used to Calculate Fatigue Endurance Limit (ANSI/ASME B106.1M, 1985).
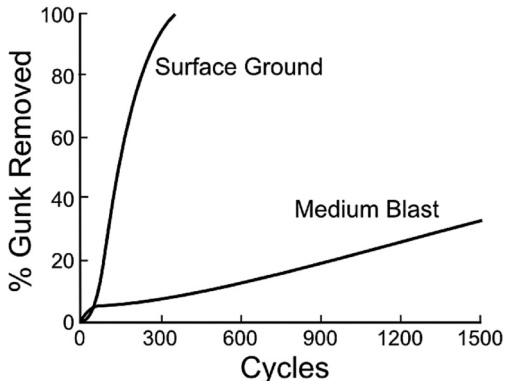
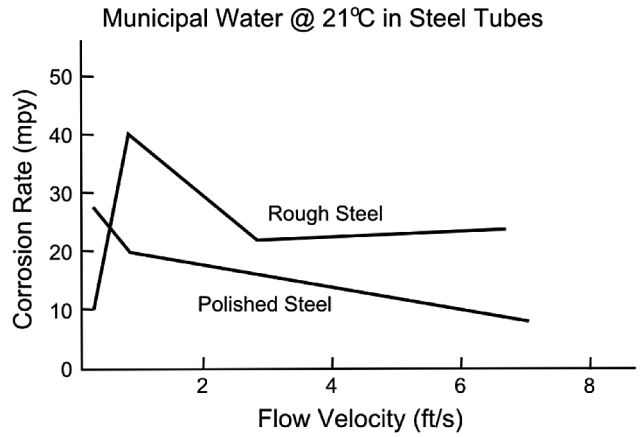

Figure 34. Effect of Surface Finish on Fouling.

Figure 35. Effect of Surface Finish on Corrosion Rate (Schweitzer, 2007).

Solid Particle Erosion

Solid particle erosion is the removal of material due to repeated impacts by small, solid particles (Kosel, 1992). The particles are small enough to be entrained in the process gas and if under a critical size, will be subject to the acceleration and direction changes along with the process gas as it progresses through the equipment. The variables that describe solid particle erosion are divided into three types: impingement variables, particle variables, and material variables. The primary impingement variables are particle velocity, angle of incidence, and particle concentration. Particle variables include shape, size, hardness, and friability. Hardness is also a material variable, along with other material properties such as work hardening behavior and microstructure.

Materials are often lumped into two groups based on their behavior at different impingement angles. Ductile materials have a maximum erosion rate at angles between 15 degrees and 30 degrees and the material removal is caused by deformation related mechanisms. The maximum erosion rate for brittle materials is at or near 90 degrees and involves cracks initiated by brittle fracture. This is illustrated in Figure 36, which shows a plot of erosion rate versus impingement angle for aluminum and alumina (Al_2O_3). Figure 37 shows relative erosion factors for various materials in solid particle erosion.
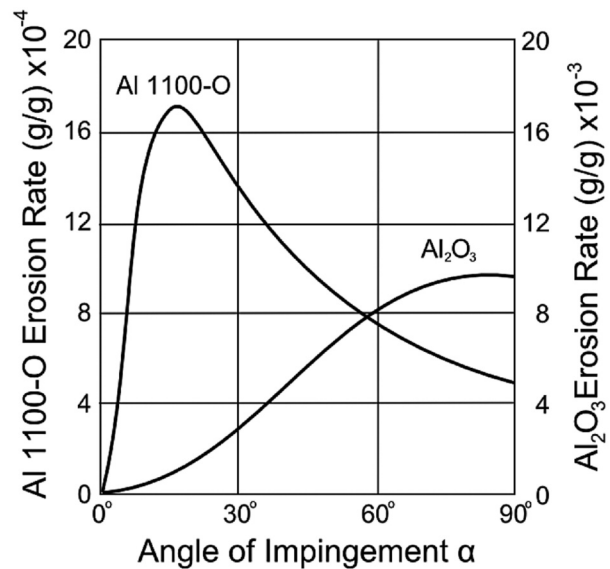

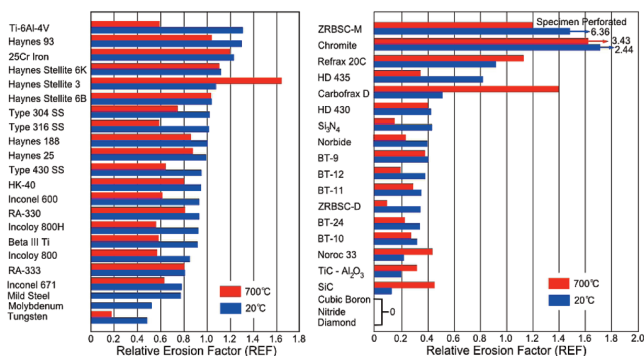Figure 36. Erosion Rate of Hard Versus Soft Materials as a Function of Impact Angle (Finnie, 1980).

Figure 37. Solid Particle Erosion Resistance of Various Materials Relative to Stellite® 6B (Hansen, 1979).

There are several phenomena that have been observed that make solid particle erosion more complicated than it appears and have implications in how to provide erosion resistance. Two of these will be discussed below in more detail.

In general, there is an inverse relationship between materials of different hardness and erosion rate (Finnie, et al., 1967). Using the data presented in Figure 38, relatively soft aluminum clearly will erode at a faster rate than 1045 steel. This seems rather obvious and is not an earth shaking finding. Things get more interesting when the data for 1045 steel is examined more closely. With increasing hardness of the same alloy, not only is there not a benefit, there is actually a slight decrease in erosion resistance. There is also only a small benefit by changing material within the same material type, as shown by the modest increase in resistance of tool steel versus 1045 steel. This has some serious implications in machines where solid particle erosion is known to be a problem. The use of another steel will not likely provide a substantial increase in erosion resistance and other alloy types are not cost effective. Therefore, erosion resistant coatings are practically a requirement rather than a luxury.
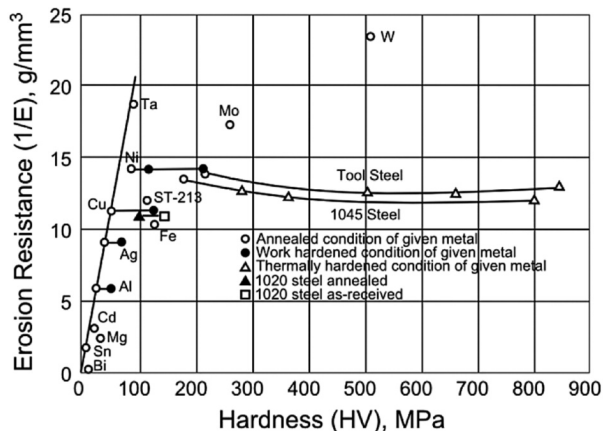

Figure 38. Solid Particle Erosion Rates of Various Materials (Finnie, et al., 1967).

The second interesting phenomenon occurs in materials with second phase particles. Materials with two phase structure where the second phase is relatively large, such as Co alloys strengthened by the formation of a carbide network, are known to have good abrasion resistance and, as will be discussed below, liquid droplet erosion resistance. Contrary to expectations, these materials do not perform well in solid particle erosion. The reason has been described as the edge effect (Kosel, 1992). If a ceramic sample is being erosion tested, it is typical that the edges of the sample round to some characteristic radius while the center is unaffected. The carbides in a Co alloy are essentially thin plates that form along the grain boundaries. The thickness of these "plates" is less than the characteristic radius, which means the formation of the radius will cut through the plate and lead

to pieces of carbide chipping off (Figure 39). The loss of the carbide chip results in an increase in the erosion rate. The edge effect is not observed in structures that have small second phases such as precipitation hardened alloys and steels.
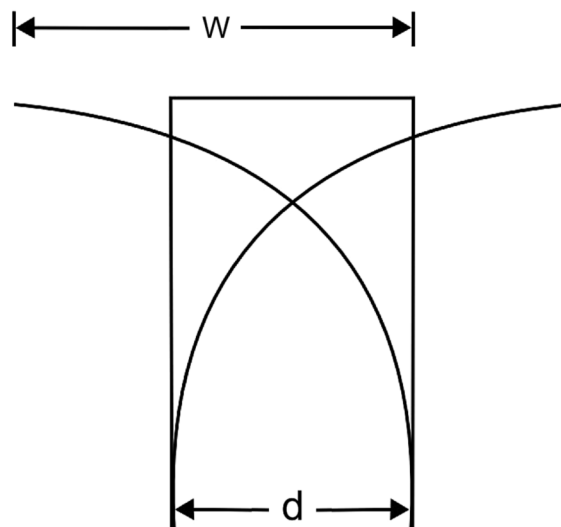

Figure 39. Illustration of Solid Particle Erosion Edge Effect (Kosel, 1992).

The most commonly encountered solid particle erosion resistant coatings are cemented carbide coatings. These coatings take into account the mechanisms and observed phenomena discussed above to provide excellent performance. Cemented carbide coatings consist of a dispersion of small particles of hard carbide, typically tungsten or chromium carbides, in a matrix of cobalt or nickel/nickel-chromium alloy. The carbide particle size (0.039 to 0.12 mils) is small enough that the edge effect that plagues Co alloys is not an issue. The small size and close proximity of the particles, which can be touching or nearly touching, means that impacting particles will often hit multiple carbides and the carbides can transmit the energy to adjacent carbides (Kosel, 1992). The matrix material also plays a role in the effectiveness of the coating. The carbides act to constrain the matrix similar to what occurs in a precipitation hardening steel, thereby increasing the yield strength significantly. Even though the yield strength is increased, the matrix retains enough ductility to help absorb and transfer some of the impact energy by plastic deformation. This is particularly important if the impact causes the carbide to crack. The ability of the matrix to plastically deform arrests the crack, limiting the extent of the damage and reducing the erosion rate.

There are not a large number of techniques for applying codeposited coatings, particularly where the two materials are vastly different in a number of properties. The application also demands good bonding between the materials and with the substrate with as little effect on the substrate as possible. Cemented carbides are therefore applied by various thermal spray techniques. The coating begins as a powder, which is fed into a torch or gun to heat the particles and then accelerated toward the part by a gas stream. The combination of heat and stress from impact causes the powder to deform into thin "splats," which adhere to the surface, overlap, and interlock as the coating gains thickness. Very little heat is transferred to the part. For wear applications, techniques with high energy input, such as high velocity oxyfuel (HVOF) or detonation gun (D-gun), are the most commonly used. These techniques provide very high densities and cohesive strength, which have been shown to improve performance of wear resistant coatings. Figure 40 shows a tungsten carbide-cobalt coating applied by HVOF. These coatings have very high hardnesses. The coating shown in Figure 40 has a hardness range of 900 to 1100 HV (~67 to 70 HRC).
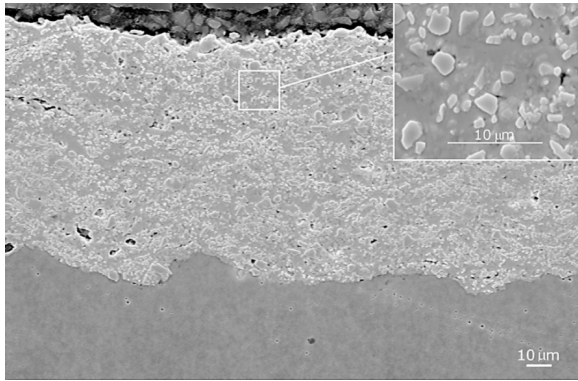
Figure 40. Photomicrograph of a Tungsten Carbide-12 Percent Cobalt Coating Applied by HVOF.

Solid particle erosion can occur in centrifugal compressors. Although it can occur in any compressor, significant solid particle erosion is most commonly encountered in single-stage blowers. The solid particles are present due to impurities in the process gas or carryover from an upstream process. Ideally, the impellers and stationary components in the gas path should be coated. Tungsten or chromium carbide coatings are frequently used. The dark areas in Figure 41 are a tungsten carbide coating on a component on a single-stage compressor. This is not always possible given the access to internal gas paths of smaller diaphragms and closed impellers. In this case, the material can be changed to a more erosion resistant material, such as a nickel-chromium alloy, or erosion resistant diffusion coatings (Figure 42).
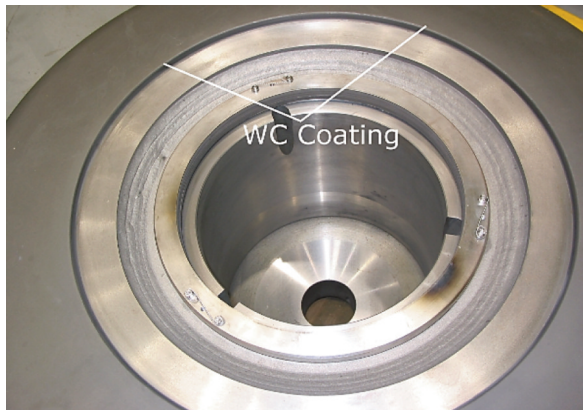

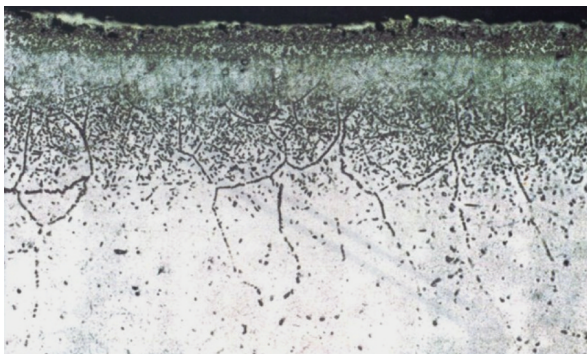*Figure 41. Tungsten Carbide Coating on a Compressor Component.*

Figure 42. Photomicrograph of a Proprietary Solid Particle Erosion Resistant Diffusion Coating.

The front end of steam turbines is also subject to solid particle erosion. The solid particles are typically due to exfoliation of oxide scales from upstream boilers and piping. Once again, the cemented carbide coatings can be used, with chromium carbide being the more commonly used due to the improved corrosion resistance at high temperatures. Figure 43 is a plot showing the benefit of chromium carbide versus uncoated 12%Cr stainless steel. Other coatings that can be used are diffusion coatings such as nitriding or boriding. Boriding, in particular, is useful where conditions are such that a phenomenon known as erosion-corrosion occurs (Fichtl, 1981). Erosion-corrosion is the synergistic interaction of erosion and corrosion that enhances the degradation rate relative to each individually. Boriding is a diffusion process where the part is heated in contact in a boron containing media. Boron diffuses into the part and hardens the steel similar to carbon or nitrogen, but to a much higher extent. The result is a case with a depth of up to 0.002 inches and hardnesses up to 1800 HV (~80 HRC) (Davis, 1994). The thin diffusion coating is an integral part of the component and can easily transfer energy upon impact by solid particles. Borided parts also have increased corrosion resistance, particularly in alkali media or dilute acids (Fichtl, 1981). Figure 44 shows a cross section of borided AISI 422 stainless steel.
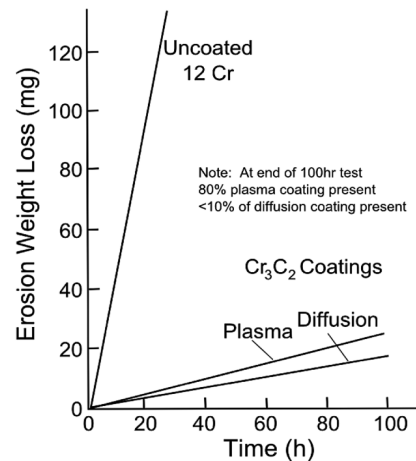

Figure 43. Solid Particle Erosion Rates of Chromium Carbide Coatings and AISI 403 Stainless Steel (Viswanathan, 1989).
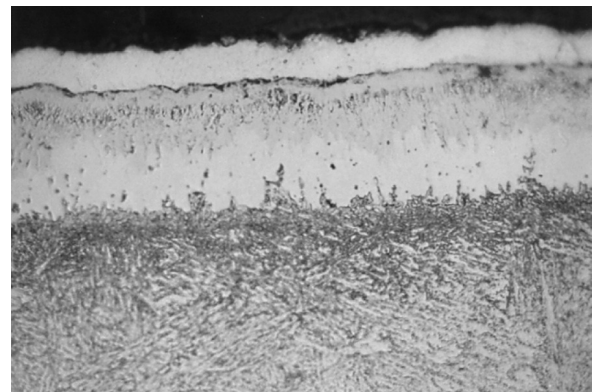

Figure 44. Photomicrograph of Borided AISI 422 Stainless Steel.

Liquid Droplet Erosion

It is obvious by its name that the nature of the erosive media involved with liquid droplet erosion differs from the solid particles discussed above. Liquid droplets tend to be larger. This increased size means that the actual velocity of the droplet is fairly low when compared to the velocity of a solid particle or even the process gas. Due to this, liquid droplet erosion is not as likely to occur on stationary components. Therefore, forces required to cause damage arise from parts moving at high velocity impacting the droplet rather than the droplet itself.

The actual mechanics behind liquid droplet erosion are somewhat complex (Heymann, 1992), not fully understood, and are beyond the scope of this paper; therefore, a very simplified description (Figure 45) will be given to aid in understanding the

reasoning for the materials used in liquid droplet erosion control. During the impact, a shockwave is created in the liquid, causing liquid to compress as it collapses against the solid surface. Eventually the liquid at the solid surface is compressed to the point that it creates a lateral jet. The shockwave in the liquid is accompanied by stress waves that propagate into the solid. This is an impulsive response, which means the reaction of the solid will depend on dynamic rather than static properties. This will have implications in the types of materials used to resist liquid droplet erosion.
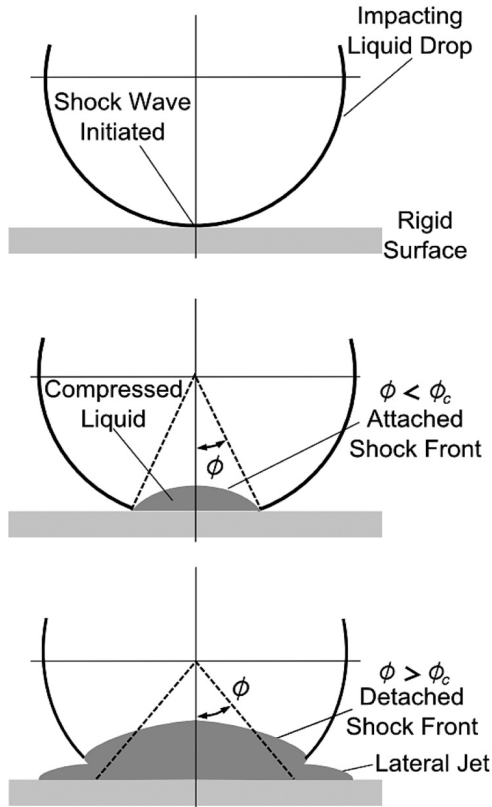

Figure 45. *Idealized Diagram of the Early Stages of Liquid Droplet Erosion (after Heymann, 1992).*

Liquid droplet erosion differentiates itself further from solid particle erosion in the manner in how it progresses over the long term (Heymann, 1992). Under constant impingement conditions, the erosion rate is very nonlinear and is characterized by several stages, as illustrated in Figure 46. The first stage is the incubation stage. The erosion rate is very low as the material is being damaged microstructurally via gradual deformation and work hardening. The impacts cause the surface to have a dimpled morphology. Eventually, enough damage is accumulated that cracks begin to form and fragments of material are removed. Because the erosion rate is rapidly increasing, this is called the acceleration stage. The acceleration stage leads up to the maximum rate stage. Here, the erosion rate has reached a steady state. At this point, the unique nature of liquid droplet erosion begins to appear, as the erosion rate drops off in the deceleration stage. When the erosion rate drops to a certain value (often ¼ to ½ the maximum rate), a steady state is reached in the terminal stage. The erosion rate remains constant indefinitely. Figure 47 shows turbine blades from the same unit after ~400 hours service and ~70,000 hours service, which illustrates the nonlinear nature of liquid droplet erosion. The reason for the rate decrease prior to reaching the terminal stage is not well understood. It is possible that the surface properties of the material change and decrease the erosion rate. Some theories are related to the surface roughening. The increased surface area associated with the roughness may require more energy to continue erosion (Heymann, 1967). The drops also

would impact peaks or slopes of the roughened surface, which reduces the impact pressure. A final theory is that liquid retained in the erosion craters counters the subsequent liquid impacts.
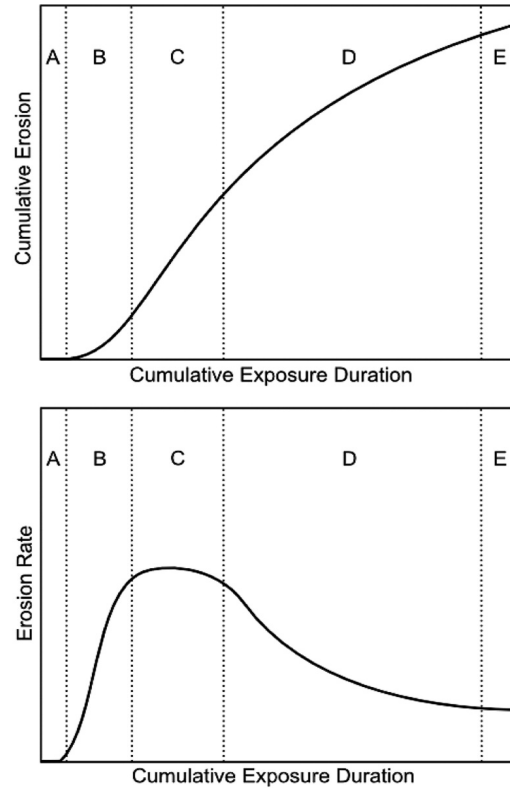

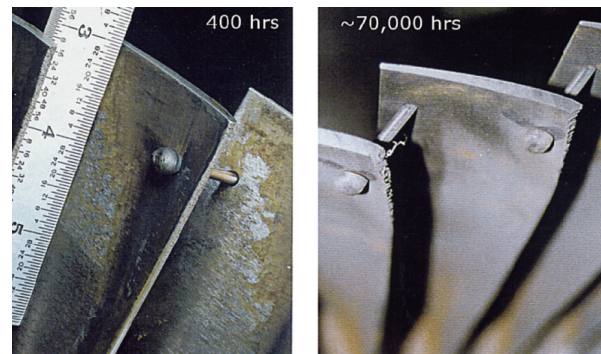Figure 46. *General Trends of Liquid Droplet Erosion Data for Turbine Blades (after Heymann, 1992).*

Figure 47. *Liquid Droplet Erosion on Turbine Blades after 400 Hours and 70,000 Hours.*

Although it can happen, it is rare for liquid droplet erosion to occur in a centrifugal compressor. Common practice is to take steps to prevent the appearance of liquids in a compressor and to minimize the droplet size should it be unavoidable. Compressor impellers also have much more open space, which means there is a lower probability of impacting a leading edge and impacts further along the impeller blade are not likely to occur at a sufficient angle (erosion rates are at a maximum with a 90 degree impingement angle) to cause significant damage. Compressor diaphragms also provide a torturous path that larger droplets cannot follow; therefore, if liquid droplet erosion is to occur, it will do so more readily near locations where they are introduced into the machine (i.e., inlets, side loads, or locations where condensation might occur). Figure 48 shows the leading edge of a first stage impeller where water was introduced into the machine without being atomized. As seen in the image, the liquid droplet erosion damage led to fatigue failure. Because it is rare for liquid droplet

erosion to occur, there are not any coatings for compressors that the authors' are aware of specifically designed for that purpose. As part of the development for a turbine antifoulant coating, the cavitation resistance (cavitation is generally considered to be a similar damage mechanism to liquid droplet erosion) of several coatings has been evaluated, including the electroless nickel antifoulant coating for compressors described above and found it did in fact provide increased resistance when compared to the base metal. Electroless nickel would also aid if the presence of liquid leads to fouling or corrosion. Given the typical access issues with impellers and diaphragms, spray coatings or weld overlays are not likely to be possible.
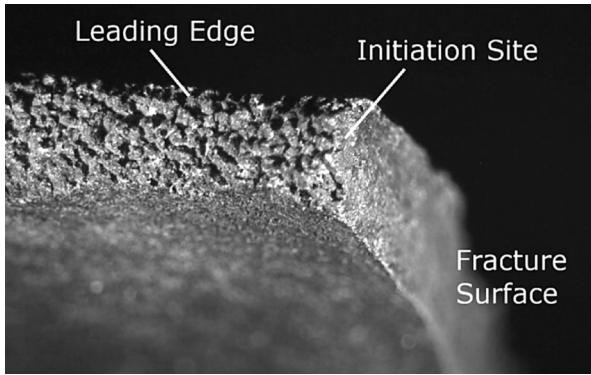

Figure 48. Liquid Droplet Erosion on the Leading Edge of an Impeller Blade Leading to a Fatigue Fracture.

Liquid droplet erosion is a well-known problem in steam turbines, particularly those that are considered condensing. At the back end of the turbine, the steam expands to the point that the temperature and pressure are such that liquid water begins to condense. Contrary to the compressor impeller, steam turbines have many tightly spaced blades; therefore, there is a low probability that a droplet will pass through a blade row without being impacted by a blade. Due to the shape of the blade, the leading edge of the blade is the location with the highest probability of impacting the drop with the required angle to cause damage. Because the damage is usually limited to the leading edge, it was found to be more cost effective to use a composite blade typically consisting of a 12%Cr stainless steel blade with a liquid droplet erosion resistant shielding/coating at the leading edge than to manufacture the entire blade from the resistant material. The shielding materials that are most commonly used are Co alloys or tool steel. Surface hardening treatments, such as flame hardening, have also been used with some success. Figure 49 shows the performance of various materials in liquid droplet erosion conditions.
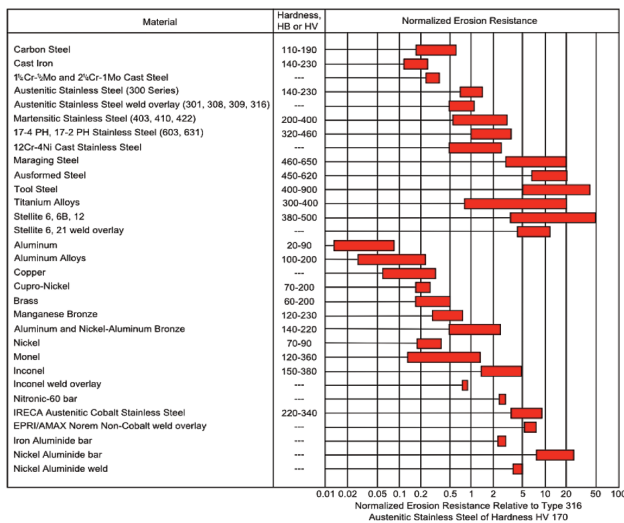

Figure 49. Performance of Various Materials under Liquid Droplet Erosion (Heymann, 1992).

The most frequently used type of material used to increase liquid droplet erosion resistance are Co-Cr-W-C alloys. These alloys form a multiphase microstructure with a cobalt-chromium matrix with a dispersion of chromium and tungsten carbides. There are some aspects of the matrix phase that make cobalt alloys the material of choice for this application. Elemental cobalt has a hexagonal crystal structure at low temperatures and changes to a cubic structure at temperatures above 782.6 °F (Davis, 2001). In the Co-Cr-W-C alloys, the transformation from face centered cubic to hexagonal occurs extremely slowly upon cooling. The unstable fcc structure gives the alloy two interesting features that give it good resistance to liquid droplet erosion. The first is that there is limited fatigue damage under cyclic loading. This extends the time for material to be removed from the surface after deformation. The second feature is that mechanical stress can induce the transformation from fcc (Figure 18) to hexagonal close packed or hcp (Figure 50). This transformation expends energy; therefore, allowing the alloy to essentially absorb some of the energy of the impacts. It is actually believed that these two features play a larger role in the excellent liquid droplet erosion resistance of these alloys than the hard carbides. Figure 51 is a comparison of Stellite® 6B, which is of the most frequently used cobalt alloys for this application, with AISI 403 stainless steel blade material after the same exposure to liquid droplet erosion. The plot in Figure 52 shows the depth of cavitation erosion damage for 48 hours of testing per ASTM G32 for various alloys, including Stellite® 6 and Haynes (Stellite®) 6B.
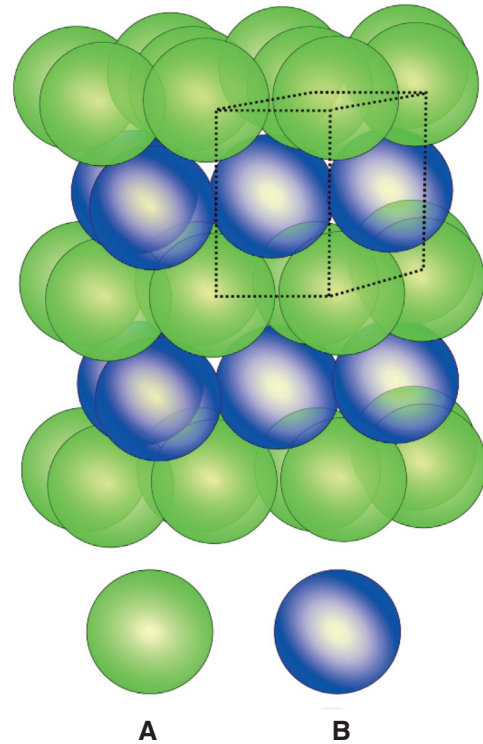

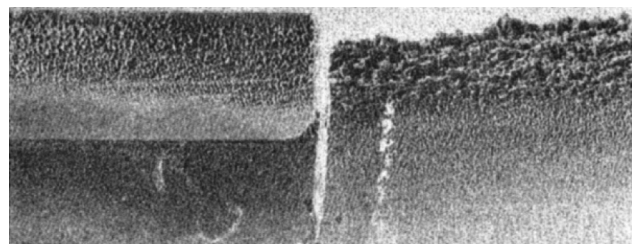*Figure 50. Hexagonal Close Packing of Atoms (after Allen and Thomas, 1999).*

Figure 51. Performance of Stellite® 6B and AISI 403 Stainless Steel in the Same Liquid Droplet Erosion Conditions (Heymann, 1992).
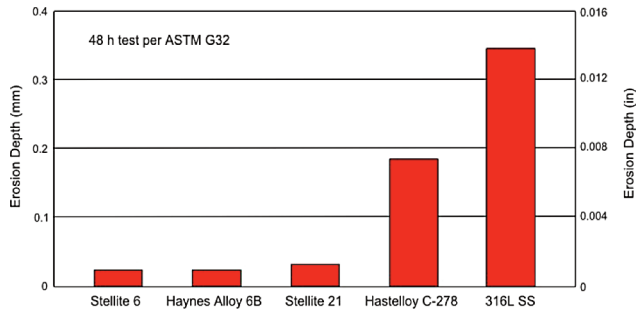
Figure 52. Depth of Cavitation Erosion Damage for 48 Hours of Testing per ASTM G32 for Various Alloys (after Crook, 1990).

There are two methods used to apply these alloys to turbine blades. The less complicated is to braze a strip of the alloy in the shape of the leading edge into a pocket machined into the blade. Brazing is a joining technique that uses a filler metal with a melting point below the materials being joined. The braze metal, typically silver for high temperature applications, is melted and pulls the two pieces together by capillary forces. The liquid also diffuses into the two parts, which binds them together upon cooling. While this method has been used with success, the strength of the joint is dependent on the thin layer of braze metal and can be further compromised by the formation of any new phases due to the diffusion of the braze metal into the joined materials. Stellite® 6B, 6K, and Stellite® 6 P/M are typical alloys that are used for brazed shields. The microstructure of these materials is shown in Figures 53 to 55 and Table 4 lists the properties. The alloys can also be applied by welding, which will put the material in the as cast condition. The welding processes typically used are plasma transfer arc (PTA) welding and laser welding. Gas tungsten arc welding (TIG) and shielded metal arc welding (SMAW) have also been used in the past. These processes are used due to the fact that they are high energy processes and can have low penetration. They heat the alloy wire or powder to a liquid so rapidly that very little heat is transferred to the blade material. This results in a small heat-affected zone in the blade material, very little dilution or interdiffusion between the alloys, and less distortion in blade. The metallurgical bond between the materials is very strong and greatly reduces the chance of the Co alloy from being removed. Figures 56 to 58 show various stages of applying Stellite® 6 to a turbine blade, along with a typical cross section and microstructure. The properties are included in Table 4. The welding method is the current standard used by some OEMs to apply these alloys.
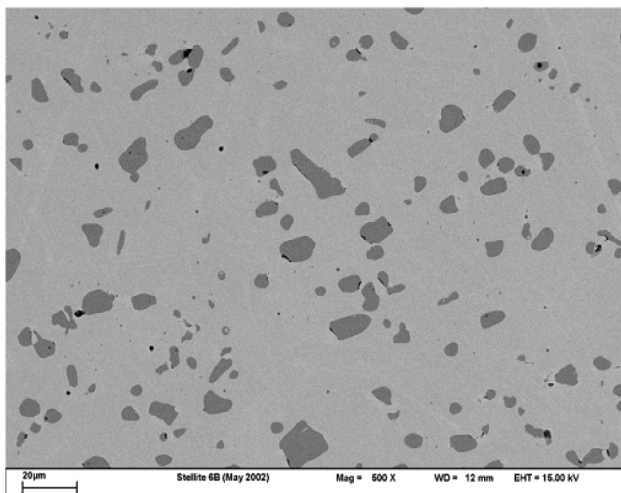

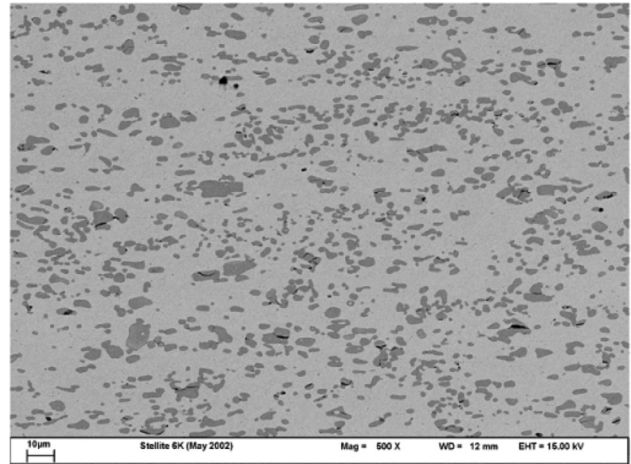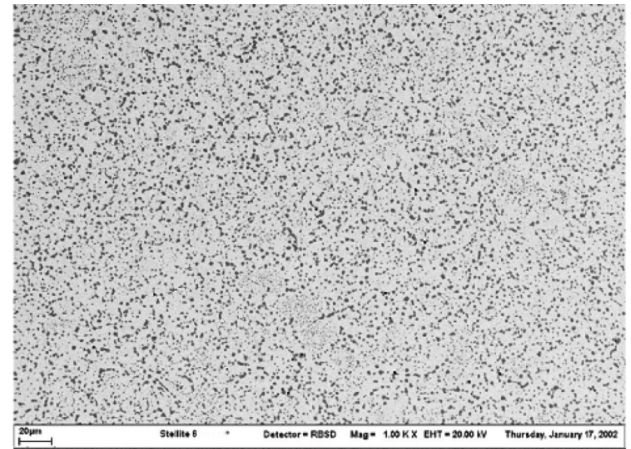*Figure 54. Microstructure of Stellite® 6K (Stellite® 6 Alloy, 2007).*

Figure 55. Microstructure of Stellite® 6 P/M (Stellite® 6 Alloy, 2007).

Table 4. Mechanical Properties of Cobalt-Based Wear Resistant Alloys (after Crook, 1990).

Property	Alloy					
	1	6	12	21	6B	T-800
Hardness, HRC	55	40	48	32	37(a)	58
Yield Strength, MPa (ksi)	---	541 (78.5)	649 (94.1)	494 (71.6)	619 (89.8)(a)	---
Ultimate Tensile Strength, MPa (ksi)	618 (89.6)	896 (130)	834 (135.5)	694 (100)	998 (145)(a)	---
Elongation, %	<1	1	<1	9	11	---
Thermal Expansion Coefficient, µm/m*°C						
From 20 to 100°C (68-212°F)	10.5	11.4	11.5	11.0	13.9(b)	---
From 20 to 500°C (68-930°F)	12.5	14.2	13.3	13.1	15.0(b)	12.6
From 20 to 1000°C (68-1830°F)	14.8	---	15.6	---	17.4(b)	15.1
Thermal Conductivity, W/m*K	---	---	---	---	14.8	14.3
Specific Gravity	8.69	8.46	8.56	8.34	8.39	8.64
Electrical Resistivity, µΩ*m	0.94	0.84	0.88	---	0.91	---
Melting Range, °C (°F)						
Solidus	1255 (2291)	1285 (2345)	1280 (2336)	1186 (2167)	1265 (2309)	1288 (2350)
Liquidus	1290 (2354)	1395 (2543)	1315 (2400)	1383 (2521)	1354 (2470)	1352 (2465)

(a) 3.2 mm (1/8 in) thick sheet. (b) Starting temperature of 0°C (32°F)

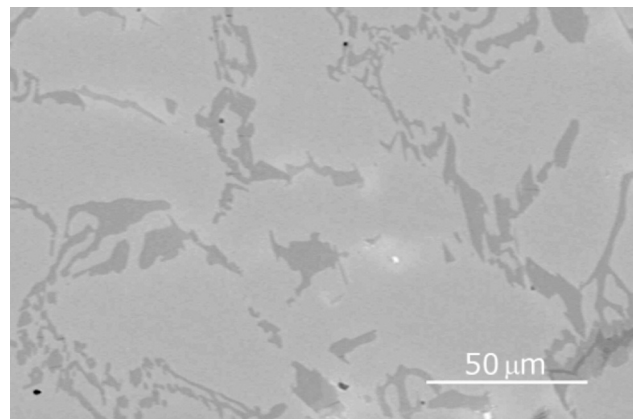*Figure 53. Microstructure of Stellite® 6B (Stellite® 6 Alloy, 2007).*

Figure 56. Microstructure of Welded Stellite® 6.

Figure 57. Cross-Section of a 403 Stainless Steel Turbine Blade with Stellite® 6 Weld Overlay.
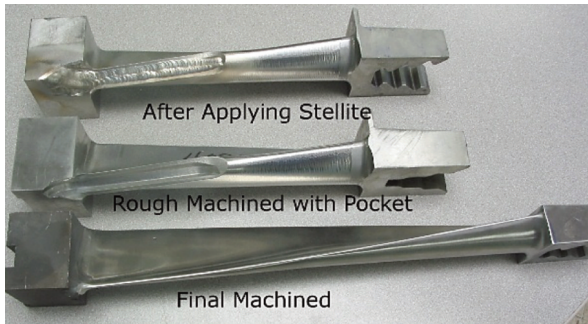

Figure 58. Various Stages of Application of Stellite® to Turbine Blades by Welding.

Tool steels are a group of steels used in the forming and cutting of other materials. Depending on the intended use of the grade, it may contain increased amounts of carbon, chromium, tungsten, molybdenum, vanadium, cobalt, and manganese (Bayer, 1990). The compositions of tool steels are tailored to optimize the balance of strength, toughness, wear resistance, and resistance to softening at temperature for the given application. It appears to be convention in literature related to liquid droplet erosion to use the generic term tool steel rather than give a specific grade. Smith, et al. (1966), mention an unnamed alloy with a composition in the range of the tungsten high speed steels (T grades). The tungsten high speed steels are designed for the high temperatures associated with high speed cutting. They contain 11 to 19 percent tungsten, which helps give the high speed steel their characteristic high red hardness and wear resistance. They are able to be full hardened to a hardness of 65 HRC or higher in parts 3 inches thick or less. Figure 59 shows the microstructure of T1 tool steel. The structure contains various carbides in a matrix of tempered martensite.
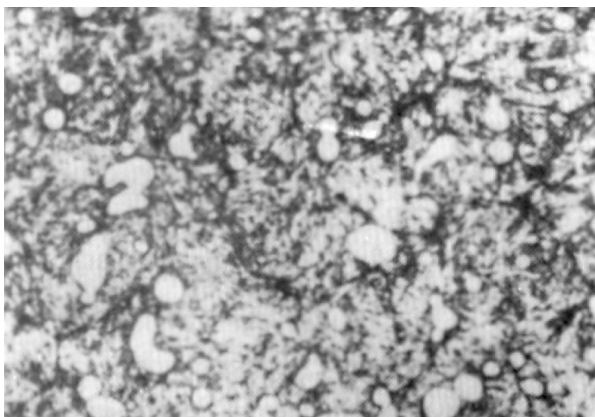
Despite the fact that Figure 51 shows that the tool steels provide as good or better resistance to liquid droplet erosion than the Co alloys, the use of tool steels for this application is infrequent. The reason is that the composition of these alloys, particularly the high carbon contents, make them difficult to apply by welding. Therefore, wrought strips of tool steel must be brazed. Similar to the wrought Co alloys above, the brazed joint is considered to be inferior to the welded Co alloys.

Another approach that has been used is to flame harden the blades. Turbine blades are frequently made from 12%Cr stainless steels that have the martensitic structure. Quenched and tempered martensitic structures offer a good combination of strength and toughness, but also present the ability to adjust the properties depending on the thermo-mechanical processing. Flame hardening is essentially a localized heat treatment used to form a higher strength tempered martensite structure at the leading edge of the blade. An oxyacetylene flame is directed on blade and the area of interest is rapidly heated above the austenitizing temperature (Ruglic, 1990). Induction heating and more recently, high power lasers, have also been used to rapidly heat the material. Care should be taken, particularly with lasers, where the energy input does not result in melting of the surface of the material. The area is then rapidly cooled or quenched to form martensite. At this point, the leading edge of the blade is very hard and brittle. The blade is then reheated to a lower temperature to temper the martensite, which allows the material to regain some toughness. The time and tempering temperature, along with the composition of the alloy dictate what the final strength of the leading edge will be. For example, quenched and tempered AISI 410 or 403 stainless steel blade material will typically have a hardness in the range of ~200 to 300 HB, while a flame hardening treatment can increase the hardness of the leading edge to ~400 to 500 HB. Figure 60 shows a flame hardened leading edge and Figure 61 shows a hardness scan across a cross section. The result is a hard, tough leading edge that is an integral part of the blade material itself. The entire process is quick and relatively inexpensive.

Figure 60. Leading Edge of a Flame Hardened Turbine Blade.

Figure 59. Microstructure of Quenched and Tempered T1 Tool Steel (Metals Handbook 8th Edition, 1972)
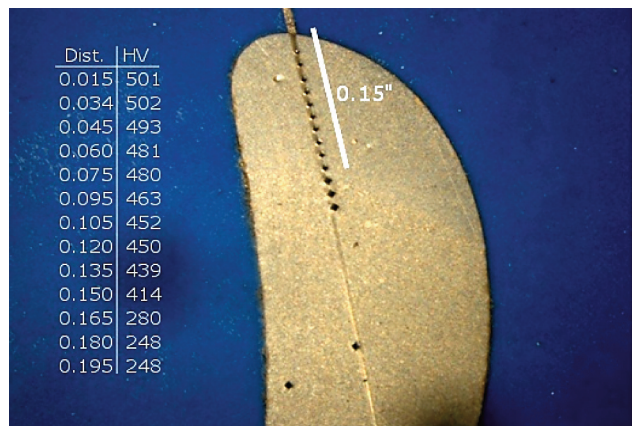
Figure 61. Cross Section and Hardness Scan of a Flame Hardened Turbine Blade.

As with all of the processes for liquid droplet erosion protection, there are some risks and trade offs. Distortion is a major issue due to the rapid heating and quenching required. Fixturing can help reduce distortion, but adds time and cost to the process. Components can also crack during quenching. Ideally, there would be a sharp temperature gradient in the material during heating and cooling to minimize or eliminate any heat affected zones, similar to what can occur during welding. This is not always possible when trying to control distortion. Depending on conditions, the hardened material may also be more sensitive to stress corrosion or hydrogen cracking in service.

RUNOUT

The term runout, in its intended form, is a measure of the out of roundness of a shaft. There are various techniques to measure runout, but the industry standard for measuring shaft runout in turbomachinery is by the use of eddy current proximity probes. These probes are noncontact, obtaining a signal from changes in the gap between the probe and shaft by monitoring the eddy currents generated by the rotating shaft material. The response is rapid and the resolution is high, making the technique nearly ideal for measuring out of roundness or vibrations in rotating equipment. The major advantage, as well as downfall of the technique is that it depends on electrical and magnetic properties of the shaft material. This means that the probe is not affected by environmental concerns such as oil mist as is typical of other techniques. On the negative side, any nonuniform properties in the shaft will alter the measurements. This can lead to identical results for a shaft that is grossly out of round, but with uniform properties and a perfectly round shaft with nonuniform properties (Figure 62) (Littrell, 2005). Very rarely is a shaft going to be at either of these extremes, and therefore the probe will measure a mixture of both mechanical (out of round or vibration) and electrical (material nonuniformity) runout.
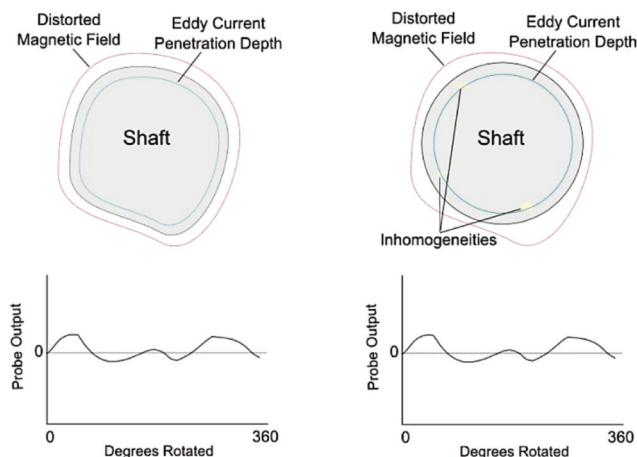

Figure 62. Diagram Showing the Same Proximity Probe Response for Cases of High Mechanical Runout and High Electrical Runout.

In large rotating equipment, low (ideally zero) levels of mechanical runout are essential for safe, long time operation. Electrical runout plays little to no role in terms of the operation of the unit. OEMs are typically required to follow API 670 (2000), which states total runout must be below 0.25 mils. The amount of either type of runout is not readily known without other measurements such as a direct contact dial indicator. If the runout happens to be higher, the route required to resolve the problem is not clear. Typically, the shaft is burnished in order to reduce the electrical runout and remachined for mechanical runout. This does not always result in a reduction in the runout, and can increase the runout if not performed properly. For the results from the eddy current proximity probe to be useful, the two types of response must be separable or the electrical component must be eliminated. This would ideally occur without the need for further processing or black box magic, whereby the probe circuitry is modified to attempt to eliminate the electrical response.

Electrical runout (ERO) can arise due to several reasons, some of which are essentially unavoidable. The chemical makeup of the material can cause ERO. Typically ERO due to chemistry comes about from a nonhomogeneous distribution of the alloying elements. This may be from segregation during casting or exposure to elevated temperature. Materials that contain precipitates and multiple phases by design are prone to high levels of ERO. A classic example of this is 17-4 PH (Littrell, 2005), where the proximity probe is affected by the difference in properties between the stainless steel matrix and the copper bearing precipitates. Forming operations (forging, rolling, drawing, grinding, etc.) and heat treating can lead to ERO by causing metallurgical textures and large grain structure variations. Residual magnetism from magnetic particle inspection, for example, can cause ERO. Actions that result in impacts on the shaft, such as peening or mishandling of the shaft, cause unseen damage on the microstructural or even atomic levels that may cause increased levels of ERO. Virtually every operation, from melt shop to installation at the customer site, can lead to ERO in some way.

Fortunately, there are ways to minimize or eliminate the electrical portion of the runout. Below is a list of several precautionary measures and techniques for mitigating ERO (Littrell, 2005).

- Proper material selection
- Careful control of melt and forging practices
- Careful handling of the shaft to minimize "bruising"
- Burnishing
- Peening (shot, ultrasonic, etc.)
- Grit blasting
- Degaussing
- Changing probe gap
- Coating or sleeving the probe area

It is important to note that most of these are not effective on all occasions and in some instances, can cause an increase in the ERO. Care must be taken during any operation to reduce electrical runout and the mechanism by which the technique reduces the ERO should be well understood.

The overall concept of how a coating can mitigate ERO can be best understood by first discussing how the proximity probe works. The probe usually contains two coils: an active coil and a balance coil to complete a bridge circuit (Doebelin, 1989). Alternating current (AC) current passing through the active coil induces a magnetic field. When the magnetic field is in proximity to a conductive target, such as a shaft, electrical currents with a circular flow pattern or eddy currents appear in the shaft. These eddy currents in turn induce a magnetic field in opposition to that of the active coil. Due to the fact that the eddy currents are induced currents, they have a low penetration into the material, meaning they are strong near the surface and drop off rapidly with depth. The penetration of eddy currents into a material is dependent on several factors, including the electrical conductivity and magnetic permeability of the material, as well as the test frequency. Changes in the distance between the shaft and probe/coil cause the strength of the eddy currents to change causing the magnetic field from the shaft to change. This alters the inductance of the active coil, leading to a change in the impedance (analogous to resistance) and an unbalance in the bridge circuit. The unbalance voltage is processed to a direct current (DC) output that is proportional to the gap size. This means there is a linear relationship between the voltage output and the gap size, with mechanical runout being a measure of the deviations in gap size. It is assumed the conductivity and permeability are essentially constant in a material. If, for example,

there are precipitates in the material that have sufficiently different electrical conductivity, the probe will react to the deviant material, causing electrical runout.

For steel, the material property values are such that the penetration is rather small and any "defects" must be very close to the surface. The small penetration depths explain why surface modification by something like burnishing can have an effect on ERO. It also allows for the use of coatings to mask the substrate material. If the coating is thicker than the penetration depth for a given coating material, the proximity probe will be influenced by the coating material only and not "see" the bulk material underneath. This is illustrated in Figure 63. Figure 64 shows a plot of the depth of penetration versus frequency for various materials. This plot can be used to determine the maximum depth that a "defect" can be in a material and be detected by the probe, as well as the minimum thickness that a coating must be to mask a substrate. As an example, using a frequency of 10 kHz, a steel coating would need to be ~5 mils, copper ~10 mils, aluminum ~50 mils, and titanium ~90 mils to mask the substrate material.
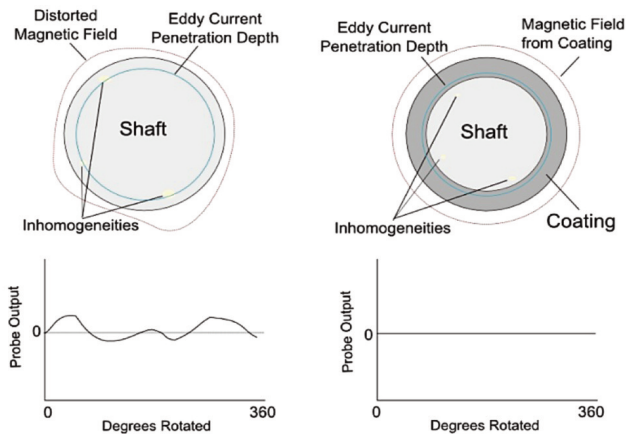

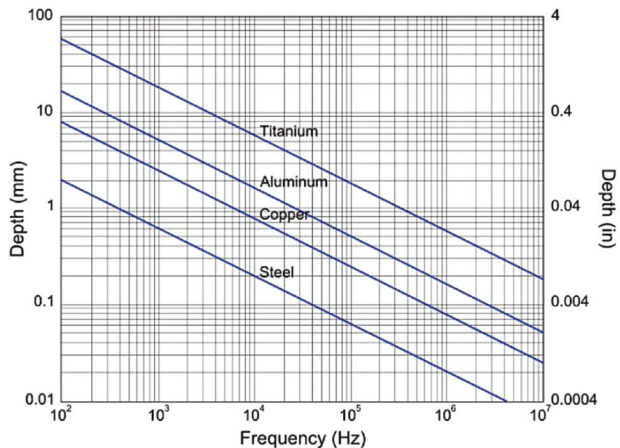Figure 63. Schematic Diagram Showing the Effect of Coatings on ERO.

Figure 64. Plot of Eddy Current Penetration Depth Versus Test Frequency for Various Materials.

When selecting a material for a coating, more must be considered than just the penetration depth. As mentioned above with respect to 17-4 PH, the material must have uniform properties. If there are precipitates or phases with significantly different properties than the matrix material, the fields may vary enough that the probe will detect the change as ERO. A high density coating of a pure element is the ideal coating, due to the fact that there is a much smaller risk for variations in properties. Pure elements also have the higher electrical conductivities than alloys, which helps reduce the penetration depth. Some alloys may be desirable due to the fact that they can have better magnetic properties. The application technique should be able to produce a clean, high density, and adherent

coating, which is easier to accomplish with a pure element. The adherence may be helped by using lighter materials that would be subject to lower stresses during operation. The material must be compatible with the shaft material and the environment in the probe area of the equipment. For example, the use of copper is frequently restricted in compressors. The material should also be machinable to the tight tolerances and finishes required. Ideally, the material would be resistant to scratches or other damage that may occur during installation or process upsets, as the probe will detect the damage. Finally, the cost of the material should be considered. Nickel has been used for this application, but is currently on the order of 10 times the price of aluminum. It may be possible to reduce cost by finding a suitable alloy with low alloy content.

WIRE WOOLING

The selection of shaft materials is also important to prevent certain types of failures, in particular, wire wooling. Wire wooling is an infrequent, but devastating, failure mechanism that occurs during startup (not necessarily the initial startup) in the bearing and seal area shafts. Areas where oil films are thin and loads are high, such as at the thrust bearing, are most susceptible to this type of failure. The process of wire wooling begins when a small particle of foreign material enters the bearing or seal. Through a series of localized temperature increases, due to high coefficient of friction between particle and rotor, material transfers from the rotor to the particle, and by hardening mechanisms, the particle becomes a hard, black scab that is able to cut and spin material from the shaft. Shaft material also continues to transfer to the scab as the cutting is occurring, allowing the scab to grow and propagate the failure. The result is a deeply grooved shaft. The material cut from the shaft often has the appearance of wire wool. Figure 65 shows damage to the journal due to wire wooling and the corresponding black scab on the journal bearing (Figure 66). For a more detailed description of the mechanism, the reader is directed to Fidler (1971).
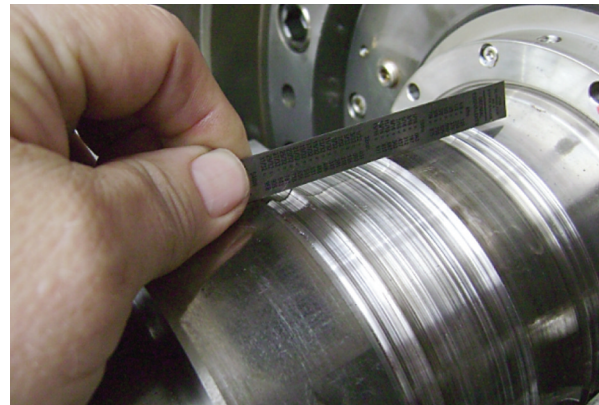

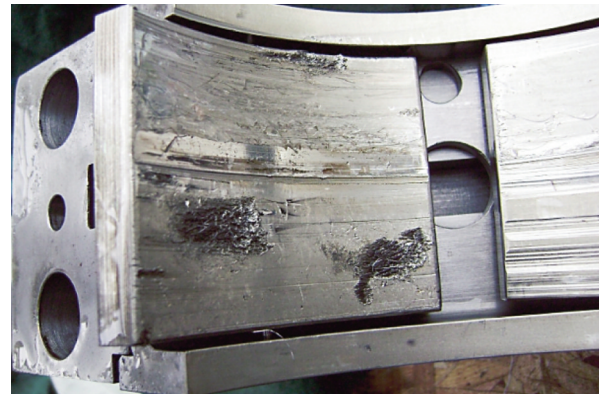Figure 65. Wire Wooling on a Compressor Shaft Journal.

Figure 66. Black Scab on the Journal Bearing Corresponding to Wire Wooling in Figure 65.

For reasons that are not clearly understood, shaft materials with higher Cr contents are more susceptible to wire wooling. The critical Cr content proposed by Fidler is 1.8 percent. Because of this, shafts should be made of 4140 or 4340 wherever possible. If a higher Cr content material must be used, steps must be taken to reduce the risk of wire wooling. Altering the surface of the shaft or increasing clearances are ways that can be used to reduce the risk. One way to alter the surface of the shaft is to harden it by nitriding or hardfacing with hard chrome or carbide coatings. Figure 67 shows a journal coated with chromium carbide. The hardness of the coating in most cases should be harder than any particles that become trapped, resulting in wear of the particle rather than machining of the shaft. Sleeving with a wire wooling resistant material, such as 4140, can also work. Increasing the clearances reduces risk by increasing the size of particle able to initiate the failure. All of these have their pros and cons, which must be evaluated when deciding which method yields the best overall results.
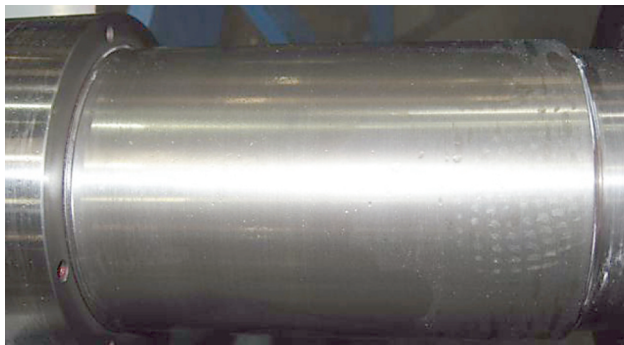

Figure 67. Images of a Chromium Carbide Coated Journal.

CONCLUSIONS

Current trends, such as increasing severity of process gases and increasing material costs, make it fairly clear that coatings will become much more prevalent in the turbomachinery industry in the future. Given this, it would be prudent for OEMs, coating applicators, and end users to be aware of what is currently available and to keep an eye open to coatings advances, because there are several interesting developments that may find a place in centrifugal compressors and steam turbines in the future. This can range from the continuous improvement of the coatings discussed above to the introduction of relatively new developments, such as nano technology, into the industry.

REFERENCES

Allen, S. and Thomas, E., 1999, *The Structure of Materials*, New York, New York: John Wiley and Sons.

ANSI/ASME Standard B106.1M, 1985, "Design of Transmission Shafting," The American Society of Mechanical Engineers, New York, New York.

API Standard 612, 2005, "Petroleum, Petrochemical and Natural Gas Industries—Steam Turbines—Special-Purpose Applications," Sixth Edition, American Petroleum Institute, Washington, D.C.

API Standard 617, 2002, "Axial and Centrifugal Compressors and Expander-Compressors for Petroleum, Chemical and Gas Industry Services," Seventh Edition, American Petroleum Institute, Washington, D.C.

API Standard 670, 2000, "Machinery Protection Systems," Fourth Edition, American Petroleum Institute, Washington, D.C.

Arney, T. and Duncan, R., 1985, "The Effect of Electroless Nickel Coatings on the Galvanic Corrosion of Other Metals," Gardner Publications, Inc., pp. 31.

Baldwin, C. and Such, T., 1968, "The Plating Rates and Physical Properties of Electroless Nickel/Phosphorus Alloy Deposits," *Transactions of the Institute of Metal Finishing*, *46*, (2), p. 73.

Baudrand, D., 1994, "Electroless Nickel Plating," *ASM Handbook Volume 5: Surface Engineering*, ASM International, Materials Park, Ohio, pp. 291-310.

Bayer, A., 1990, "Wrought Tool Steels," *ASM Handbook Volume 1: Properties and Selection: Irons, Steels, and High Performance Alloys*, ASM International, Materials Park, Ohio, pp. 757-779.

Chessick, J., Healey, F., and Zettlemoyer, A., 1956, "Adsorption and Heat of Wetting Studies of Teflon," *Journal of Physical Chemistry*, *60*, (10), pp. 1345-1347.

Chow, R., McMordie, B., and Wiegand, R, 1994, "Performance Maintenance of Centrifugal Compressors Through the Use of Coatings to Reduce Hydrocarbon Fouling," Elliott Company, Reprint: R-264.

Crook, P., 1990, "Cobalt and Cobalt Alloys," *ASM Handbook Volume 2: Properties and Selection: Nonferrous Alloys and Special Purpose Materials*, ASM International, Materials Park, Ohio, pp. 446-454.

Davis, J., 2001, "Nickel, Cobalt and Their Alloys," ASM International, Materials Park, Ohio.

Davis, R., 1994, "Surface Engineering of Stainless Steels," *ASM Handbook Volume 5: Surface Engineering*, ASM International, Materials Park, Ohio, pp. 741-761.

Doebelin, E., 1989, *Measurement Systems Application and Design*, Boston, Massachusetts: McGraw-Hill Higher Education.

Dowson, P., 2007, "Antifoulant and Corrosion Resistant Coatings for Cracked Gas Compressors and Steam Turbines," AICHE Spring National Meeting, Houston, Texas.

Dowson, P., Bauer, D., and Laney, S., 2008, "Selection of Materials and Material Related Processes for Centrifugal Compressors and Steam Turbines in the Oil and Petrochemical Industry," *Proceedings of the Thirty-Seventh Turbomachinery Symposium*, Turbomachinery Laboratory, Texas A&M University, College Station, Texas, pp. 189-209.

Ebara, R., Nakajima, H., Odohira, T., Wada, T., and Hatano, M., 1987, "Application of Ion-Plated Cr-TiN Multilayer Coating to Steam Turbine Blades," *Proceedings for the Sixteenth Turbomachinery Symposium*, Turbomachinery Laboratory, Texas A&M University, College Station, Texas, pp. 3-8.

Electroless Nickel Plating, http://www.thelindgrengroup.com/electroless_nickel_plating.html, Accessed May 18, 2010.

Fichtl, W., 1981, "Borinizing and Its Practical Applications," *Materials and Design*, *2*, (6), pp. 276-286.

Fidler, F., 1971, "Metallurgical Considerations in Wire Wool Type Wear Bearing Phenomenon," *Wear*, *17*, pp. 1-20.

Finnie, I., 1980, "The Mechanisms of Erosive Wear in Ductile Materials," *Corrosion-Erosion Behavior of Materials*, K. Natesan, Editor, TMS-AIME, pp. 118-126.

Finnie, I., Wolak, J., and Kabil, Y., 1967, "Erosion of Metals by Solid Particles," *Journal of Materials*, *2*, pp. 682-700.

Fluoropolymer Comparison—Typical Properties, http://www2.dupont.com/Teflon_Industrial/en_US/tech_info/techinfo_compare.html, Accessed February 20, 2010.

Garverick, L., 1994, *Corrosion in the Petrochemical Industry*, ASM International, Materials Park, Ohio.

Gawrilow, G., 1979, *Chemical (Electroless) Nickel Plating*, Red Hill, England: Porticullis Press.

Graham, A., Lindsay, R., and Read, H., 1965, "The Structure and Mechanical Properties of Electroless Nickel," *Journal of the Electrochemical Society*, *112*, (4), p. 401.

Hansen, J., 1979, "Relative Erosion Resistance of Several Metals," *STP 664: Erosion: Prevention and Useful Applications*, ASTM, pp. 148-162.

Heresite Protective Coatings Inc., 1999, Manitowoc, Wisconsin.

Heymann, F., 1967, STP408: *On the Time Dependence of the Rate of Erosion Due to Impingement or Cavitation*, ASTM, pp. 70-110.

Heymann, F., 1992, "Liquid Impingement Erosion," *ASM Handbook Volume 18: Friction, Lubrication and Wear Technology*, ASM International, Materials Park, Ohio, pp. 221-232.

Kosel, T., 1992, "Solid Particle Erosion," *ASM Handbook Volume 18: Friction, Lubrication and Wear Technology*, ASM International, Materials Park, Ohio, pp. 199-213.

Laney, S. and Walker, M, 2009, "Application of Pos-E-Coat 523 to Assembled Compressor Rotors: Final Report," Elliott Company, Project D18908-03.

Littrell, N., 2005, The Color of Runout, *Orbit*, *25*, (3), pp. 4-17.

Maloney, J. L. III, 1992, "Friction and Wear of Tool Steels," *ASM Handbook Volume 18: Friction, Lubrication and Wear Technology*, ASM International, Materials Park, Ohio, pp. 739.

Metals Handbook 8th Edition, Volume 7: Atlas of Microstructures of Industrial Alloys, 1972, American Society for Metals, Metals Park, Ohio, p. 118.

NACE Standard MR0103, 2007, "Standard Material Requirements—Materials Resistant to Sulfide Stress Cracking in Corrosive Petroleum Refining Environments," NACE International, Houston, Texas.

NACE Standard MR0175/ISO 15156, 2003, "Petroleum and Natural Gas Industries Materials for Use in H2S-Containing Environments in Oil and Gas Production," NACE International, Houston, Texas.

NEMA Standard SM-23, 1991, "Steam Turbines for Mechanical Drive Service," National Electrical Manufacturers Association, Rosslyn, Virginia.

Parker, K. and Shah, H., 1971, "Residual Stresses in Electroless Nickel Plating," *Plating*, *58*, (3), p. 230.

Piper, G. and Wang, J., 2007, "Selective Plating System," U.S. Patent: US 2007/0284256 A1.

Ruglic, T., 1990, "Flame Hardening," *ASM Handbook Volume 4: Heat Treating*, ASM International, Materials Park, Ohio, pp. 268-25.

Schweitzer, P., 2007, *Corrosion Engineering Handbook, 2nd Edition*, Boca Raton, Florida: CRC Press.

Smith, A., Caldwell, J., McAllister, D., and Christie, D., 1966, "Physical Aspects of Blade Erosion by Wet Steam in Turbines [and Discussion]," *Philosophical Transactions of the Royal Society A*, 260, pp. 209-219.

Stallman, K. and Speckhardt, H., 1981, "Deposition and Properties of Nickel-Boron Coatings," *Metalloberfl Angewandte Elektrochemie*, *35*, (10), p. 979.

Stellite® 6 Alloy, 2007, Deloro Stellite.

Stickels, C.A., 1992, "Carburizing," *ASM Handbook Volume 18: Friction, Lubrication and Wear Technology*, ASM International, Materials Park, Ohio, pp. 873-876.

Sturley, R. and Moore, S., 1982, "Compressor Coatings Project, Final Report: Anti-Stick and Compatibility Test Results," Carrier Corporation, Project E170-11.

Viswanathan, R., 1989, *Damage Mechanisms and Life Assessment of High Temperature Components*, ASM International, Materials Park, Ohio, p. 319.

Wang, W., Dowson, P., and Baha, A., 2003, "Development of Antifouling and Corrosion Resistant Coatings for Petrochemical Compressors," *Proceedings of the Thirty-Second Turbomachinery Symposium*, Turbomachinery Laboratory, Texas A&M University, College Station, Texas, pp. 91-97.

Watson, A. P., Carter, D. R., and Alleyne, C. D., 1995, "Cleaning Turbomachinery Without Disassembly, Online and Offline," *Proceedings of the Twenty-Fourth Turbomachinery Symposium*, Turbomachinery Laboratory, Texas A&M University, College Station, Texas, pp. 189-209.

ACKNOWLEDGEMENT